CHAPTER VI
CONVERSION OF METHYLESTERS OVER CsNaX ZEOLITE CATALYST

6.1 Abstract

The deoxygenation of methyl octanoate over a CsNaX zeolite catalyst has been investigated as a model reaction for the production of hydrocarbons from biodiesel. Several operating parameters were investigated, such as the type of basic catalyst used, the co-reactant incorporated in the reactor as a solvent of the liquid feed, and reaction temperature. The CsNaX zeolite catalysts used in the study was prepared by ion exchange of NaX with 0.1 M of $CsNO_3$ solution. A significant role of the co-reactant was found on the activity, selectivity, and stability of the catalyst. That is, when methanol was co-fed enhanced stability and decarbonylation activity were observed. By contrast, when nonane was used, the catalyst deactivated rapidly and the selectivity to coupling products was enhanced. Temperature programmed desorption (TPD) of methyl octanoate and methanol, as well as flow catalytic studies suggest that methyl octanoate first decomposes to an octanoate-like species. The decomposition of such species leads to the formation of heptenes and hexenes as major products. Octenes and other hydrogenated products are formed in lower amounts via hydrogenation by hydrogen produced on the surface by methanol decomposition, but not from gas phase H_2, followed by dehydration. A significant amount of Cs cation was eliminated after the washing leading to the loss of basic strength. Hexenes are produced as main product over these washed CsNaX catalysts. Moreover, it was found that Cs cation did not enhance the additional decarbonylation activity. When the polarizable Cs cation is not present in the catalyst reduced activity and formation of undesired products, such as aromatics and pentadecanone, occur. Similarly, the highly polar environment within the micropores of the zeolite X seems to enhance the activity greatly, whereas non-zeolitic basic catalysts, such as MgO, exhibit low activity.

Keywords: Basic zeolites, CsNaX, Biofuels, Methylesters, Deoxygenation, Decarbonylation, Deacetalation, Hydrogenation, TPD, TPRx

6.2 Introduction

The demand of renewable fuels as replacements of fossil fuel has been increasing for the past several years. Among the various biomass-derived fuel investigated, fatty acid methyl-ester biofuels (FAME) obtained by trans-esterification of triglycerides from natural oils and fats with methanol have received considerable attention [1-4]. They exhibit high cetane number and are considered to burn cleanly; however, there is growing concern about the fungibility of these fuels with petroleum-derived diesel due to the oxidative and thermal instability [5-7]. Reduction of the oxygen content in the fuel would readily improve the stability of the fuel and therefore its utilization potential. Various processes including hydrogenolysis [8, 9], decarbonylation [10, 11], and decarboxylation [12, 13] of FAME have been proposed to transform the biodiesel into the hydrocarbon base fuel.

The decarbonylation and decarboxylation have advantages over hydrogenolysis because, while the hydrocarbons thus produced may contain less carbon than its fatty acid counterpart, the former reactions require much less hydrogen than the latter [8]. Moreover, the properties of the fuel obtained by decarbonylation / decarboxylation are not significantly different from those obtained from hydrogenolysis [12]. Typically, decarbonylation takes place over the supported noble metal catalysts at relatively high temperature (> 350°C) [14]. For example, Pd/C has been found to be an effective catalyst for decarbonylation / decarboxylation [12]. However, CO produced from the reaction may competitively adsorb on the metal surface, leading to a reduction or even loss in the catalytic activity as conversion increases. Hence, total and hydrogen partial pressures are generally high, in order to keep the surface clean and facilitate the oxygenate-metal surface interaction, and reduce the catalyst deactivation [15].

An alternative family of catalysts that may overcome some of these limitations is that of solid bases. This is because the FAME is fairly electrophilic while the decarbonylated by-product, CO, is nucleophilic. Thus, while the adsorption of FAME over basic catalyst may be strong and the reaction can be readily promoted at atmospheric pressure, the by-product CO would promptly leave the basic surface. As a result, considerably lower temperature and hydrogen partial pressure may be

required. Among possible solid base catalysts, low-silica zeolites containing highly polarizable cations, such as cesium, may be good candidates. These catalysts have been found to exhibit relatively high activity towards reactions involving oxygenates [16 , 17], as well as hydrogenation and hydrogenolysis of acrylonitrile and propionitrile [18]. It has been suggested that, in addition to the need for strong basicity, an active catalyst requires the co-existence of acid and basic sites for reactions such as hydrogenation and hydrogenolysis [19]. In fact, an alkali-exchanged zeolite such as the CsNaX contains conjugate acid-base pairs, in which the exchangeable alkali cation has Lewis acidity and the oxygen that bridges Si and Al near the exchangeable cation has basicity [20].

The purpose of this work is to investigate deoxygenation reactions on Cs- and NaX zeolite catalysts using methyl octanoate as a model feed that may mimic some of the most relevant reactions involved in the refining of biodiesels. The effects of varying reaction conditions such as temperature, hydrogen partial pressure, feed concentration, presence of competing molecules, as well as catalyst formulations were investigated in a flow reactor. The washing with deionized water was applied to study the role of excess cesium. In addition, temperature programmed techniques were employed to elucidate possible reaction pathways thought to be relevant in the deoxygenation of FAME.

6.3 Experimental

6.3.1 Catalyst Preparation and Characterization

Commercial molecular sieve (UOP type 13X, NaX), MgO (LOT No. 130337), NaY (CBV 100) were obtained from Fluka, Schweizerhall, and Zeolyst, respectively. The as-received materials were calcined at 723 K and 973 K, respectively. The Cs-containing zeolite (CsNaX) was prepared by ion exchange of molecular sieve 13X with 0.1 M of $CsNO_3$ solution at 353 K for 24 h. The solid material was filtered and left to dry at 80°C overnight. The sample was then calcined at 723 K for 2 h in a flow of dry air. It was designated as CsNaX(20). The washing with deionized water was applied to the samples prepared with the same procedure as

used for the preparation of CsNaX(20). The samples after washing repeatly for 4 and 7 times were designated as CsNaX(5) and CsNaX(2), respectively. The numbers in the parenthesis represent the amount of excess cesium. It has been demonstrated that crystallinity in all CsNaX samples is largely retained after this treatment [21]. Surface areas of the CsNaX and NaX catalysts were determined by nitrogen adsorption at 77 K using a Micromeritics ASAP 2000 apparatus. X-ray diffraction (XRD, Bruker AXS D8Discover) was employed to investigate the catalyst structure. The hydrogen uptake of the catalysts was measured by Temperature Programmed Reduction (TPR) in an apparatus constructed for this purpose.

6.3.2 FTIR of Adsorbed Acetonitrile

FTIR technique was carried out to determine the basic strength of the Cs-containing NaX zeolite catalysts using acetonitrile as a probe molecule. The samples were prepared and pretreated in a flow of 2% O_2/He at 723 K for 2 h. After the pretreatment, it was cooled down to room temperature and a blank spectrum was taken. Then, the acetronitrile (10 μl) was injected to the sample cell in a flow of He. The helium gas was kept flowing for 1 h to purge the excess acetonitrile. After that, the sprectrum was taken again.

6.3.3. Temperature Programmed Desorption (TPD) of Isopropylamine

The catalyst acidity was tested by the amine TPD technique. First, 50 mg of sample was pretreated at 723 K in a flow of 2% O_2/He for 1 h. After the pretreatment, the sample was cooled in He to room temperature and then consecutive 10 μl pulses of isopropylamine (IPA) were injected to the sample until saturation was achieved, as indicated by a constant m/z=44 signal in the MS. After removing the excess IPA by flowing He for 3 h, the sample was linearly heated to 973 K at a heating rate of 10 K/min. Masses (m/z) of 44, 41, and 17 were monitored to determine the evolution of desorbing species and MS fragments. The signal 44 is only due to IPA; by contrast, 41 and 17 are due to propylene and ammonia,

respectively, but also to MS fragments of IPA. To determine whether there is desorption or decomposition, one follows the evolution of the three signals simultaneously. In this case, no decomposition was observed and the three signals kept the same ratio throughout the desorption. The amount of desorbed IPA was calibrated with 50 μl pulses of 2% propylene in He (m/z=41).

6.3.4 Temperature Programmed Desorption (TPD) of Methyl Octanoate

The evolution of pre-adsorbed methyl octanoate over CsNaX catalysts was followed by temperature programmed desorption in an apparatus equipped with a mass spectrometer (MS). In each run, 50 mg of the sample was initially pretreated in a flow of 2% O_2/He for 2 h at 723 K. Then, the sample was cooled in He flow to 423 K. A 100 μl pulse of methyl octanoate was injected to the sample, and a He flow was introduced for 3 h at 423 K in order to remove the excess methyl octanoate. The sample was then heated to 1173 K at a rate of 10 K/min. Masses (*m/z*) of 2, 28, 56, and 74 were monitored to determine the evolution of hydrogen, carbon monoxide, hydrocarbons, and methyl octanoate, respectively.

6.3.5 Temperature Programmed Desorption (TPD) and Temperature Programmed Reaction (TPRx) of Methanol

Methanol was chosen as a probe for the zeolite surface and as a co-reactant to help reduce the rate of catalyst deactivation during the conversion of methyl octanoate. Therefore, the desorption and decomposition of methanol over CsNaX and NaX catalysts were investigated by TPD and TPRx techniques in the same apparatus described in the previous section. In each run, 50 mg of the sample was initially pretreated in a flow of 2% O_2/He for 2 h at 723 K. Then, the sample was cooled in He flow to room temperature. In the desorption experiment, 10 μl of methanol was repeatedly injected over the sample at room temperature until reaching saturation, as indicated by a steady MS signal. After the removal of the excess methanol by flowing He for 3 h at room temperature, the sample was heated to 1173

K at a rate of 10 K/min. For the TPRx experiment, methanol was continuously fed through the sample bed at a flow rate of 1 ml/h. The sample was linearly heated from room temperature to 973 K at a heating rate of 10 K/min. Masses (*m/z*) of 2, 28, 31, and 45 were monitored to determine the evolution of hydrogen, carbon monoxide, methanol, and dimethylether, respectively.

6.3.6 Catalytic Activity Measurements for the Deoxygenation of Methyl Octanoate

The deoxygenation of methyloctanoate was carried out at atmospheric pressure, in a fixed bed flow reactor made with ¼ in. quartz tube. Prior to the reaction, the catalyst samples were pretreated *in situ* under flow of 2% O_2/He at 723 K for 2 h. Then, the catalyst bed was cooled to the reaction temperature (698 K) under flow of He (25 ml/min). The reactant feed of 10 %wt methyl octanoate in methanol solvent was introduced into the reactor using a syringe pump via a heated vaporization port. Alternatively, in some runs, nonane was used as a solvent instead of methanol. Unreacted feed and products were quantified using an online GC-FID equipped with a capillary HP-5 column, following a temperature program to optimize product separation.

6.3.7 Temperature Programmed Oxidation (TPO) of Coke Deposits after Reaction

The temperature programmed oxidation (TPO) was employed to investigate and quantify the nature and amount of coke deposited on the spent catalysts. 30 mg of the sample was packed in the 1/4" quartz tube reactor. The temperature was ramped to 1173 K with a heating rate of 10 K/min and the TPO profiles were recorded under flow of 2% O_2/He. The CO_2 produced by the oxidation of the coke deposits was further converted to methane over a methanation catalyst (15% Ni/Al_2O_3) in the presence of hydrogen at 673 K. The corresponding methane was then analyzed online by an FID detector. The amount of oxidized coke was calibrated using 100 μl pulses of pure CO_2 injected to the same system.

6.4 Results

6.4.1 Characterization of the Fresh Catalysts

The NaX and all of Cs-containing NaX catalysts were characterized by XRD and BET surface area analysis. The XRD pattern of all Cs-exchanged NaX catalysts showed almost the same pattern as that of NaX, which confirms that the Cs-containing NaX catalysts have the same crystalline phase after the cesium exchange and washing. However, the decreases in the peak intensity of all of the cesium exchanged NaX zeolite catalysts were observed. This lowering of peak intensity might be contributed from the difference in X-ray adsorption coefficient of the parent NaX catalyst when larger cations (Cs^+) are incorporated into the NaX zeolite catalyst [22]. The bulk (ICP) compositions of all catalysts are presented in Table 6.1. It shows that the significant amount of Cs cations of the CsNaX(20) catalyst have been exchanged with Na ions in the zeolite frameworks leading to the significant drop in BET surface area and pore volume, compared to the parent NaX zeolite catalyst. It must be noted that the CsNaX (20) catalyst was prepared without the washing treatment; hence, excess Cs cations remained on the catalyst in the bulk particles of cesium oxide, cesium carbonate, cesium peroxide, and cesium superoxide resulting in the drop in the surface area due to the pore blockage by these species. A significant fraction of the cesium species could be eliminated by the washing treatment as observed from the CsNaX(5) and CsNaX(2) catalysts. This leads to a partial recovery of surface area.

The temperature programmed reduction (TPR) was carried out to quantify the hydrogen consumption of the fresh zeolite catalysts. As shown in Figure 6.1, a significant amount of hydrogen consumption can be observed at around 823 K over the CsNaX(20) zeolites whilst no hydrogen was consumed by the NaX sample. In addition, relatively less amount of hydrogen consumption was found, when the washing treatment was applied as observed for the CsNaX(5) and CsNaX(2) catalysts. Therefore, it is clear that the high hydrogen consumption observed on the CsNaX(20) is due to the reduction of the excess cesium species. The Cs bulk species (oxides ore carbonates) may be formed from excess Cs during the activation in air

during the calcination step [23,24]. The hydrogen consumption increases with the amount of excess cesium species in the sample.

Table 6.1 Elemental analysis data of NaX and CsNaX catalysts

Catalysts	Surface area (m^2/g)	Total Composition		Excess cesium per unit cell
		Si/Al	Cs/Al	
NaX	695	1.2	-	-
CsNaX(2)	522	1.1	0.36	2.2
CsNaX(5)	439	1.2	0.40	4.9
CsNaX(20)	367	1.2	0.60	19.8

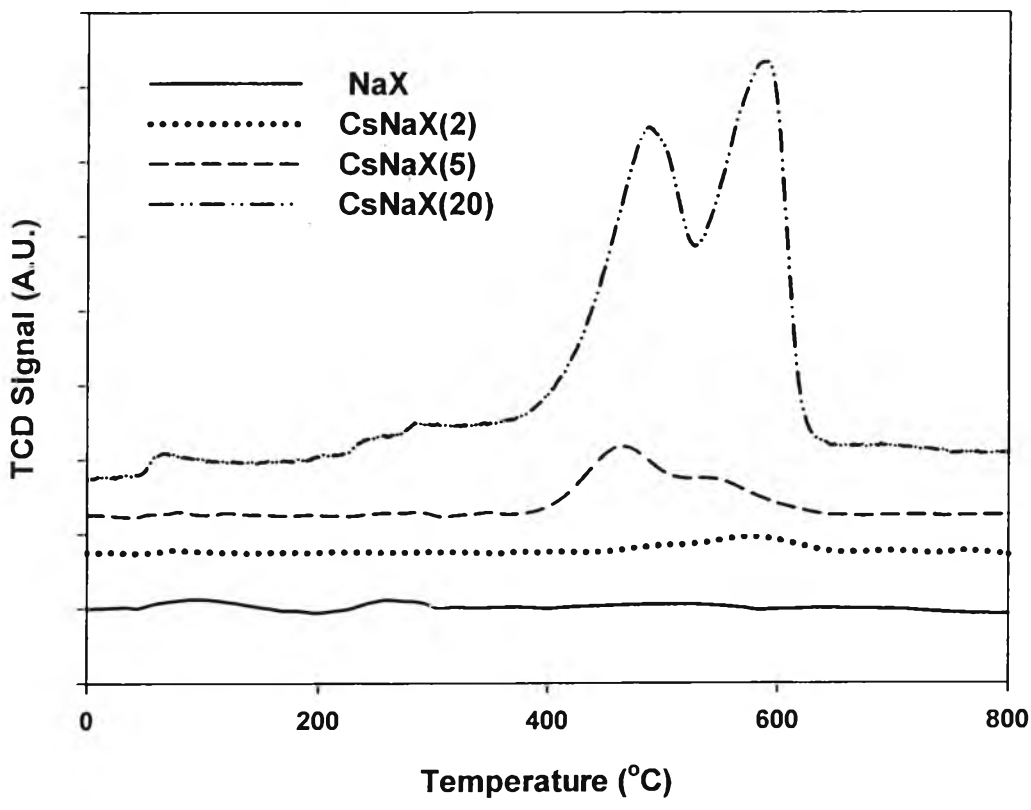

Figure 6.1 TPR profiles of the CsNaX and NaX catalysts; all of them treated in air at 723 K before starting the TPR.

6.4.2 Acid-Base Characterization of the Fresh Catalysts

The basic characteristic of all Cs-containing catalysts were analyzed by FTIR techniques using acetronitrile as probe. The adsorption band appearing at 2254 cm^{-1} is assigned to the stretching vibration frequency of C≡N group of the acetronitrile. It is anticipated that the stretching vibration frequency of the -CN group of the adsorbed acetonitrile should decrease, compared to that of acetonitrile vapor if the basic strength increases. This is because the –CN group of the adsorbed acetonitrile would be stretched when the electron density of such molecule increases with increasing in the basic strength of the active sites. Therefore, the longer –CN bond leads to the decrease in the vibration frequency of the adsorbed acetonitrile [25].

Regarding to the IR spectrum illustrated in Figure 6.2, it shows that the adsorption band of the NaX (2257 cm^{-1}) is slightly higher than that of vapor acetonitrile. As expected, the presence of cesium cations in the catalysts results in the shift of the adsorption band to lower frequency. Particularly, the frequency of the adsorption band was lowered when the cesium content in the CsNaX catalysts was decreased. This clearly suggests that the basic strengths of the CsNaX catalysts are in the order of CsNaX(20) > CsNaX (5) > CsNaX (2). As expected, the CsNaY catalyst shows less basic strength although it has the same pore structure as the CsNaX(20) catalyst. This is because of the difference in Si/Al ration between Y and X zeolites.

Consistent with this view, the TPD of isopropylamine suggested that alkali-exchanged zeolite possesses some acidity. As shown in Figure 6.3, the evolution of adsorbed IPA at lower temperature (~453 K) is responsible for the weak adsorption of IPA on the zeolite framework, while that at higher temperature may represent acid sites, but not the strong Bronsted sites typically found in HY or HZSM-5. In those cases, the isopropylamine does not desorb at high temperatures as a whole molecule, but rather it decomposes into propylene and ammonia. In the present zeolites, there is no decomposition, but rather desorption. Quantification of the desorbed amount resulted in about 2.9 $\mu mol/g_{cat}$ for the weakly adsorbed IPA on the CsNaX(20) catalyst, but no strongly adsorbed species. By contrast, on the NaX zeolite, about 4.6

μmol/g_{cat} were weakly adsorbed and 3.6 μmol/g_{cat} strongly adsorbed, which is consistent with the presence of some residual acidity on this catalyst.

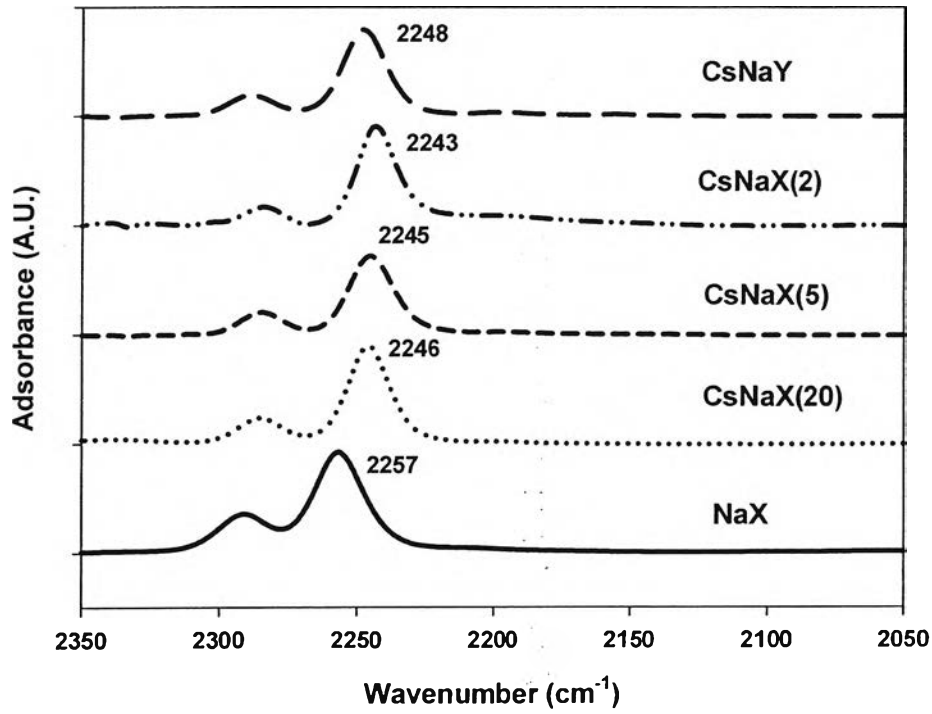

Figure 6.2 FTIR of adsorbed acetonitrile over the CsNaX and NaX catalysts.

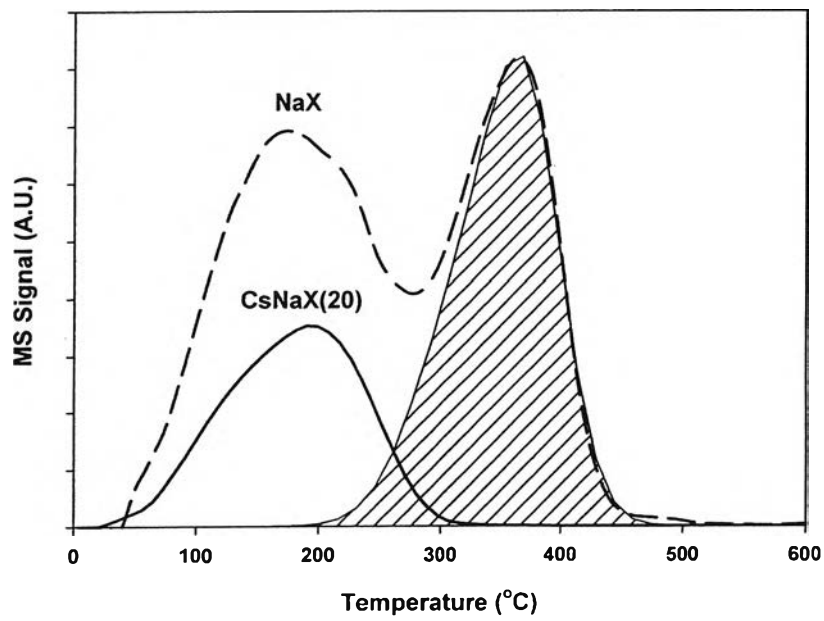

Figure 6.3 Evolution of *m/z* = 44 during TPD of isopropylamine.

6.4.3 Temperature Programmed Desorption (TPD) and Reaction (TPRx) of Methanol

The evolution profiles obtained from TPD of adsorbed methanol are shown in Figure 6.4. A significantly higher amount of undissociated methanol is desorbed from the NaX catalyst than from the CsNaX(20) catalyst. Moreover, while the NaX zeolite exhibited two desorption peaks at temperatures around 423 K and 573 K, the CsNaX(20) zeolite only had the lower-temperature peak. Similar differences in the TPD profiles of adsorbed methanol on NaX and CsNaX have been previously observed [26]. These differences were suggested to arise from a stronger interaction of the adsorbate with the Na cations in the NaX, as compared to those in the CsNaX(20). However, other adsorption studies [27, 28] would indicate that one could also assign the lower temperature TPD peak to methanol adsorption on sites located in the supercages of the NaX and the higher temperature peak to sites located in the smaller sodalite cages. The difference in binding strength in the two sites can be explained in terms of the shorter-range interactions taking place in the small cavities of the sodalite cages. Accordingly, the disappearance of the high temperature peak from the TPD of the CsNaX(20) indicates that the presence of the much larger Cs cations in the small sodalite cage dramatically reduces its accessible pore volume, thus preventing the adsorption of methanol on these sites. Based on this description, adsorption on the CsNaX(20) zeolite catalyst would occur only in the larger supercages, but even this peak is smaller than the corresponding one on the NaX, due to the larger extent of blocking by Cs

To investigate the temperature range that is more relevant to the reaction studies, the decomposition of methanol over the CsNaX(20) catalyst was examined by temperature programmed reaction (TPRx) under continuous flow of methanol. As shown in Figure 6.5(a), the decomposition of methanol starts at 573 K, and in agreement with previous studies [29], hydrogen (H_2), and carbon monoxide (CO) are the main decomposition products. However, it is interesting to note that they do not appear at the same time. To make this trend more clearly visible, the H_2/CO ratio is plotted in Figure 6.5(b). A sharp rise in this ratio is observed above 573 K, but it goes back to a constant low value at higher temperatures. This observation suggests

that methanol primarily decomposes into H_2 that desorbs and a fragment that remains on the surface. The species retained on the surface has been previously identified by ^{13}C NMR [30] and suggested to be a formate-like species. As the temperature is increased, this formate-like species can further decompose evolving CO. Beyond this temperature the continuous decomposition produces both CO and H_2.

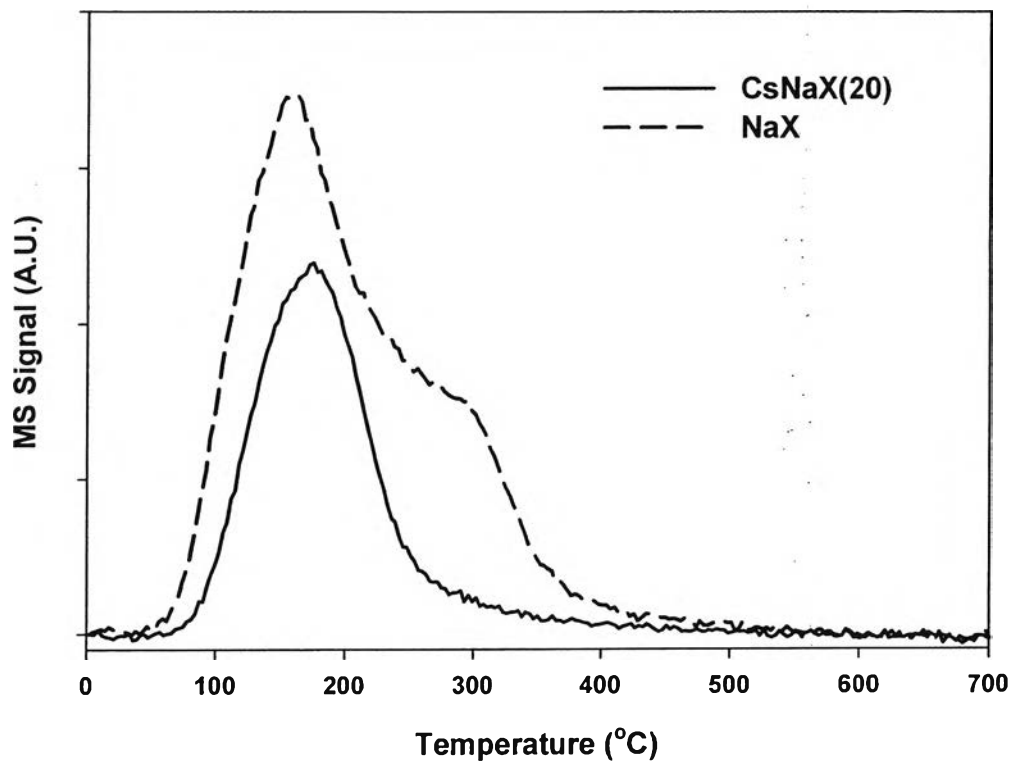

Figure 6.4 TPD profiles of adsorbed methanol over the CsNaX(20) and NaX catalysts.

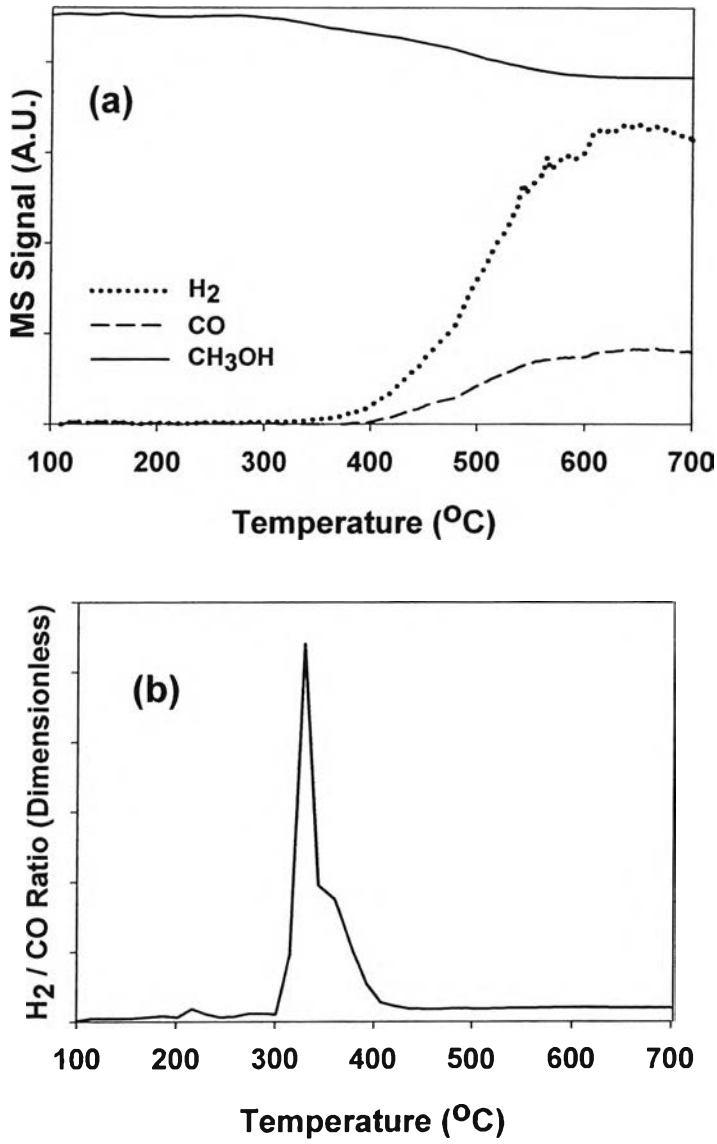

Figure 6.5 (a) Temperature Programmed Reaction of continuous flow methanol over CsNaX (b) H_2/CO signal of continuous flow of methanol over the CsNaX(20) catalyst.

The desorption characteristics of methyl octanoate over the CsNaX(20) catalyst are shown in Figure 6.6. Unlike the case of methanol, the TPD of adsorbed methyl octanoate reveals no evolution of the parent methyl octanoate molecule, suggesting that this is strongly adsorbed. Instead, decomposition products are observed. CO and H_2 were initially evolved above 573 K and 673 K, respectively.

From the areas, we have quantified the amount of CO evolved below 723 K to be about 1.6 μmol/g_{cat}. This amount of CO is produced by the decomposition of methyl octanoate at the methoxyl group. On the other hand, a larger amount, 6.8 μmol/g_{cat} of CO, is produced at temperature higher than 723 K from the decarbonylation of methyl octanoate. It is important to note that contrary to methanol, essentially no hydrogen is evolved up to about 673 K. A significant amount of hydrogen (4 μmol/g_{cat}) was only produced at 723 K.

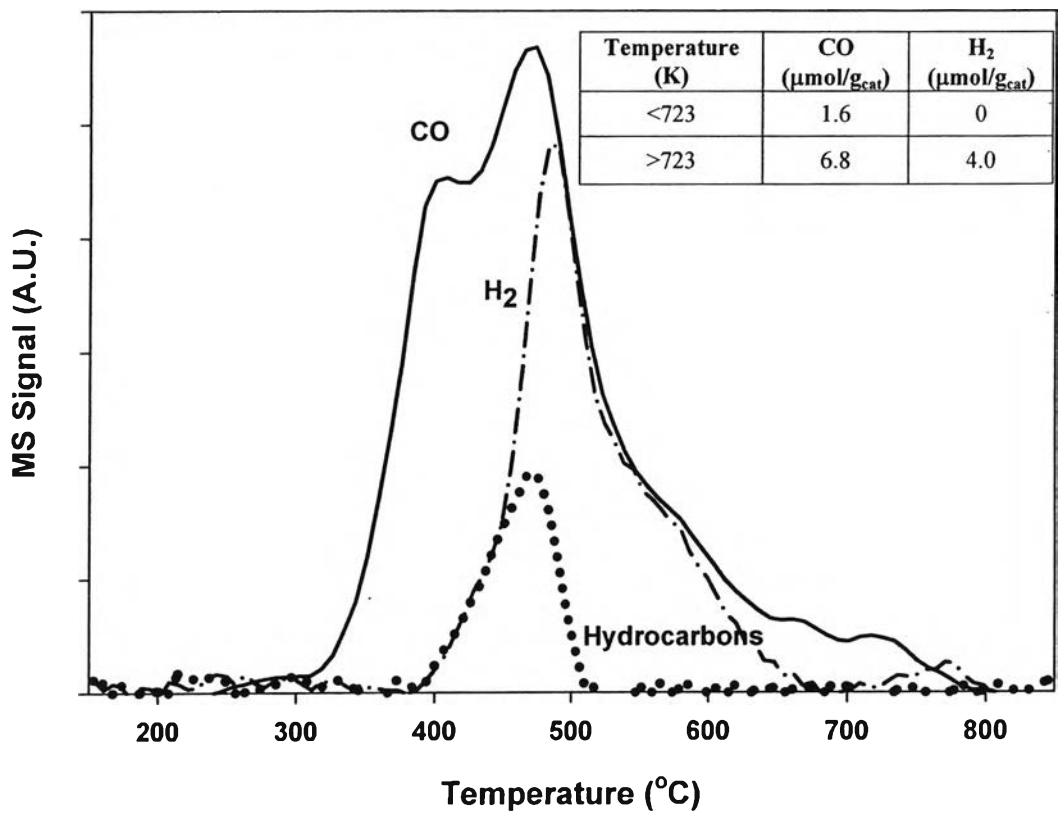

Figure 6.6 TPD profile of adsorbed methyl octanoate on the CsNaX(20) zeolite catalyst.

6.4.4 Reaction under Continuous Flow of Methyl Octanoate

6.4.4.1 CsNaX Catalysts

The effect of co-feeding methanol was investigated during the decarbonylation of methyl octanoate over the basic CsNaX(20) zeolite catalyst. The conversion from the reactions using nonane or methanol as solvent are compared in Figure 6.7. It can be seen that when nonane was used, a high activity was observed at the beginning of the reaction; however, this activity was rapidly lost by catalyst deactivation. On the other hand, while a relatively lower activity was observed when methanol was cofed into the reaction system, a much better stability with time on stream was obtained.

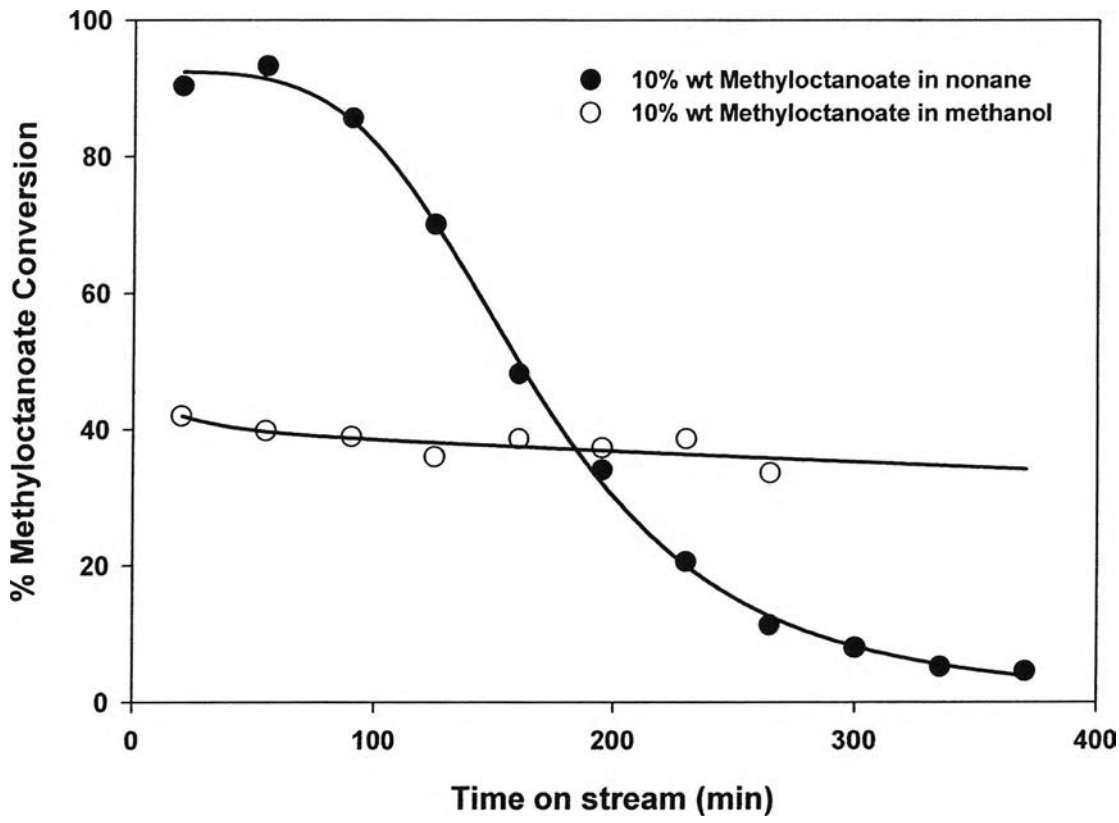

Figure 6.7 Conversion of 10 %wt methyl octanoate over the CsNaX(20) catalyst using nonane and methanol as solvent as a function of time on stream. Reaction Conditions: 698 K, 1 atm, W/F = 198 g*h/mol, 25 ml/min of He.

The product distributions from the decarbonylation of 10 %wt methyl octanoate over the CsNaX(20) catalyst using nonane and methanol as solvents are compared in Figure 6.8(a) and 6.8(b), respectively. In the reaction co-feeding nonane, the dominant product was 8-pentadecanone, a coupling product of methyl octanoate. Deoxygenated products, namely octene, heptene and hexane were also observed, but with lower selectivities. When methanol was used as a solvent, very small amounts of coupling products (i.e. 8-pentadecanone) were obtained. In this case, the reaction products were mostly heptenes, hexenes, and octenes; that is, the dominant reactions were decarbonylation (elimination of CO), deacetalation (elimination of CH_3CHO), and hydrogenation/dehydration (elimination of O). It is clear that while the conversion of methanol itself is rather low (~5%), its presence greatly affects the product distribution and stability of the catalyst.

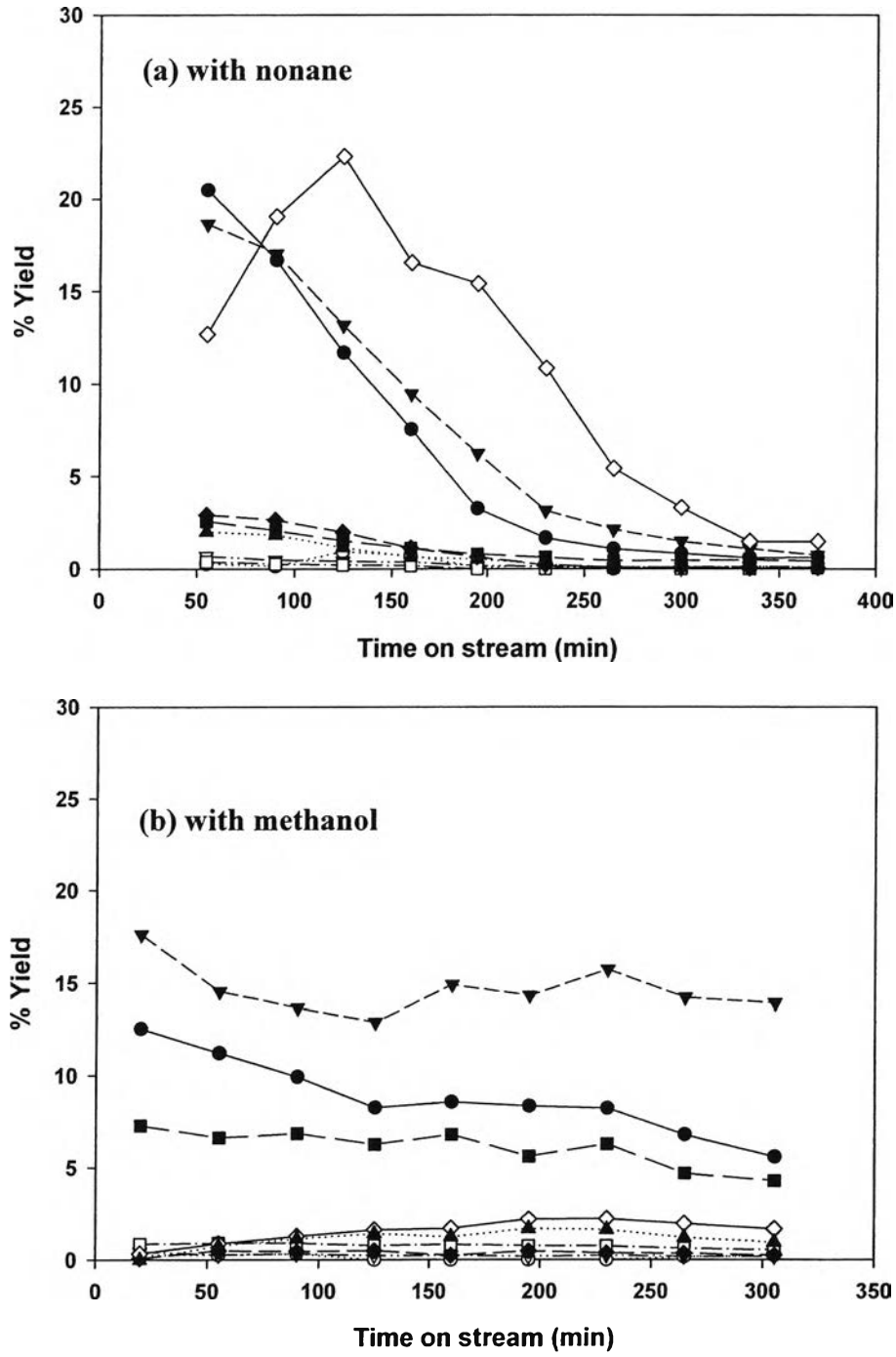

Figure 6.8 Product distributions from the reaction of 10% wt methyl octanoate over the CsNaX(20) catalyst using (a) nonane and (b) methanol as solvent as a function of time on stream. Reaction Conditions: 698 K, 1 atm, W/F = 198 g*h/mol, 25 ml/min of He. Heptenes (▼), Hexenes (■), Octenes (●), Pentadecanone (◇), Coupling ester (▲), Octane (□), Tetradecene (◆), Heptane (▽), Hexane (○).

Table 6.2 summarizes the product distribution from the reaction of 10% wt methyl octanoate in methanol at various space times (W/F). As discussed above, the major product is C_7 hydrocarbons (i.e. heptenes), which is the expected product from direct decarbonylation of methyl octanoate over the CsNaX(20) catalyst. In addition, significant amounts of hexene are obtained. As discussed below, we believe that hexenes are products of deacetalation. In significantly lower concentrations octenes and coupling products, together with small amounts of octanes and oxygenates, were also observed. As shown in Figure 6.9(a) and 6.9(b), the yields of heptenes and hexenes increase parallel to the overall conversion as a function of W/F, suggesting that both are primary products. That is, hexene is not a secondary product arising from the cracking of heptene. By contrast, as shown in Figure 6.9(b), the evolution of octene follows a different pattern; it seems to reach a plateau at an overall conversion near 40% and the start of this plateau coincides with the increase in the formation of secondary products such as lower oxygenates, octanoic acid, and tetradecene (see Figure 6.9(c)). On the other hand, the coupling products exhibit a drop in the concentration as a function of W/F, indicating that these heavier compounds tend to react further into lighter compounds as the catalyst bed increases.

Table 6.2 Product distribution from reactiom of 10 %wt methyl octanoate in methanol over the CsNaX(20) catalyst at various space time

	W/F (g.h/mol)		
	99	198	396
Conversion	24.0	37.2	62.3
Yield (%)			
Hexenes	4.5	8.8	19.3
n-Hexane	0.2	0.1	0.3
Heptenes	8.9	14.6	26.1
n-Heptane	0.1	0.2	0.8
Octenes	3.0	6.1	6.7
n-Octane	0.4	0.8	1.0
Octanal	0.6	0.5	0.4
Oxygenates	1.9	2.0	3.3
Octanonic acid	0.8	1.1	2.2
Tetradecene	0.3	0.3	0.6
Pentadecanone	2.0	1.5	0.9
Coupling ester	1.2	1.1	0.8

Reaction Conditions: 698 K, 1 atm, 25 ml/min of He.

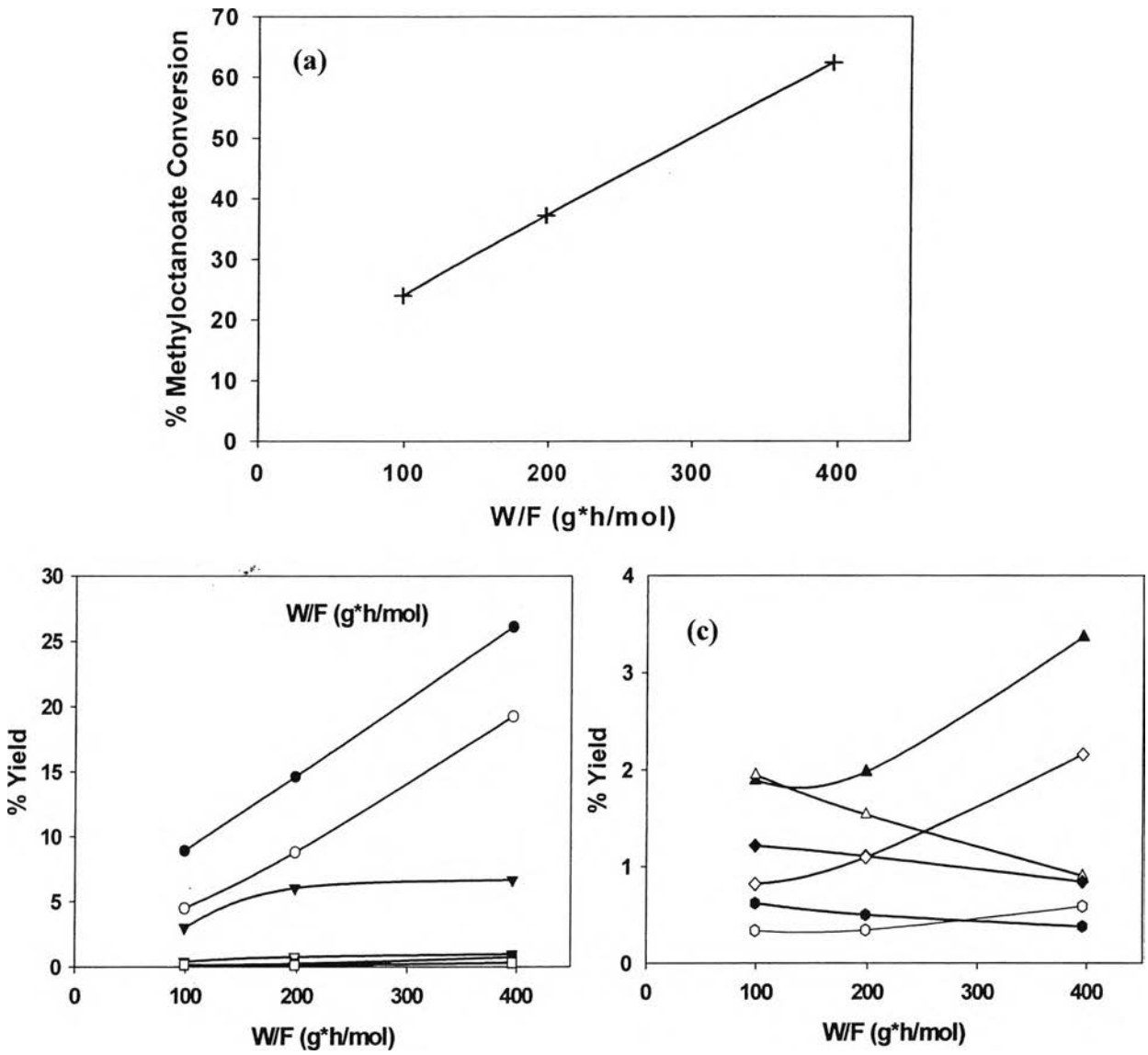

Figure 6.9 Conversion (a), yields of major products (b), yields of minor products (c) from the reaction of 10 %wt methyl octanoate in methanol over the CsNaX(20) catalyst as a function of W/F. Reaction Conditions: 698 K, 1 atm, 25 ml/min of He. Heptenes (●), Hexenes (○), Octenes (▼), Octane (▽), Heptane (■), Hexane (□), Oxygenates (▲), Pentadecanone (△), Coupling ester (◆), Octanoic acid (◇), Octanal (⬢), Tetradecene (◊).

A major consideration in the production of fuels from biomass is the consumption of hydrogen [31], which is typically needed in reactions involving deoxygenation steps. We have investigated the impact of the presence of hydrogen on the overall activity and product distribution observed in the conversion of 10 %wt methyl octanoate in methanol over the CsNaX(20) catalyst. Table 6.3 summarizes the conversion and product distribution obtained on the CsNaX(20) catalyst at various reaction conditions.

Table 6.3 Product distribution from reaction of 10 %wt methyl octanoate over the CsNaX(20) catalyst using methanol as solvent at various conditions

	Conditions		
Carrier gas	He	H_2	He
Reaction Temperature (°C)	425	425	400
Conversion	37.2	34.8	10.8
Decabonylation / Coupling Ratio	11.4	8.3	5.0
Olefin/Paraffin Ratio	25.7	24.5	14.2
Selectivity (%)			
Hexenes	23.7	22.3	20.2
n-Hexane	0.3	0.9	1.8
Heptenes	39.4	40.7	35.8
n-Heptane	0.5	0.9	1.8
Octenes	16.4	10.9	9.2
n-Octane	2.2	1.4	0.9
Octanal	1.3	2.0	1.8
Oxygenates	5.4	6.6	8.3
Octanonic acid	3.0	3.4	3.7
Tetradecene	0.8	1.1	0.9
Pentadecanone	4.0	6.0	9.2
Coupling ester	3.0	3.7	6.4

Reaction Conditions: W/F = 198 g*h/mol.

Interestingly, very similar activity, stability (not shown) and product selectivity were observed at 698 K when comparing the reaction under H_2 and under He. The main decarbonylation products, C_7 and C_6 olefins, were dominant under both gases, indicating little effect of gas-phase hydrogen in this reaction. It is also interesting to note that the octene yield obtained when using He was higher than when using H_2 as a carrier gas. This result demonstrates that the decarbonylation over the CsNaX(20) catalyst does not require gas-phase hydrogen when methanol is used as a solvent. The presence of hydrogen also had no effect on the catalyst stability, indicating that hydrogenation of carbonaceous residues does not take place.

To investigate the effect of reaction temperature, Table 6.3 includes data from a run conducted at 673 K, rather than at 698 K. At the lower temperature in He, the conversion decreases as expected compared to the same reaction at 698 K. The changes in selectivity are consistent with a higher activation energy for the decarbonylation and deacetalation reactions compared to the rest, particularly the coupling reactions. That is, while the selectivity to hexene and heptene slightly decreases at 673 K, the selectivity to the coupling products increased.

Another important aspect worth to mention is the effect of excess cesium cation of the CsNaX zeolite catalysts. The reaction of 10%wt methyl octanoate in methanol was carried out over the CsNaX(2) and CsNaX(5) catalysts at the same conditions as that on the CsNaX(20) catalyst in a flow of He. The conversion from the reaction over the different content of excess cesium species as a function of time on stream is shown in Figure 6.10. It can be seen that the CsNaX(5) catalyst initially provided a higher activity, compared to the CsNaX(20) catalyst. Then, the activity was slowly deactivated after 150 min time on stream. The similar catalytic acitivity was also observed over the CsNaX(2) catalyst.

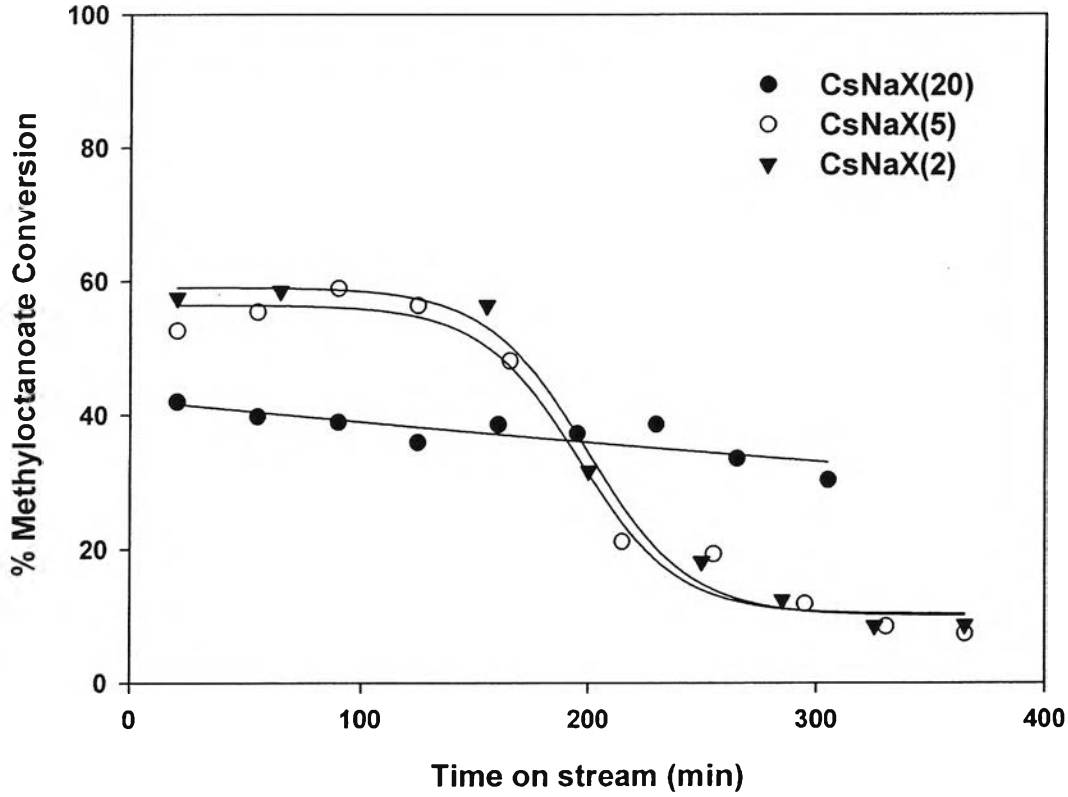

Figure 6.10 Conversion of 10 %wt methyl octanoate in methanol over the CsNaX catalysts with different excess cesium content. Reaction Conditions: 698 K, 1 atm, W/F = 198 g*h/mol, 25 ml/min of He.

The product distributions from the reactions over the various CsNaX catalysts at 20 min and 300 min time on stream are summarized Table 6.4. It was found that heptenes is the main product obtained from the CsNaX(20) catalysts, which is arise from the direct decarbonylation of the methyl octanoate. While, the selectivity to heptenes decreases with decreasing in the excess cesium contents per unit cell, the hexenes selectivity increases. Hexenes become a major product from the reaction over the CsNaX(2) catalyst, containing the least content of excess cesium. This may suggest that the increase in hexene concentration is presumably due to the formation of cyclic-like species, which takes place on the acid sites.

Moreover, the reduction of octene concentration was observed when the excess cesium concentration decreases.

Table 6.4 Product distribution from reaction of 10 %wt methyl octanoate in methanol over the various CsNaX catalysts

	Catalysts					
	CsNaX(20)		CsNaX(5)		CsNaX(2)	
Excess cesium per unit cell	19.8		4.9		2.2	
TOS (min)	20	300	20	300	20	300
Conversion	37.2	29.0	52.6	19.3	55.6	12.4
Selectivity (%)						
Hexenes	23.7	20.2	25.1	23.5	30.2	24.7
n-Hexane	0.3	0.6	2.1	1.4	10.0	2.1
Heptenes	39.4	42.6	36.4	32.8	24.1	23.3
n-Heptane	0.5	2.4	4.7	4.1	6.2	4.7
Octenes	16.4	9.5	4.7	9.1	3.6	7.0
n-Octane	2.2	1.1	1.7	1.6	1.3	1.0
Octanal	1.3	6.8	11.7	4.1	11.2	9.1
Oxygenates	5.4	1.7	2.1	1.3	1.9	2.2
Octanonic acid	3.0	2.2	3.6	6.3	3.0	4.6
Tetradecene	0.8	0.0	1.2	0.0	2.6	0.0
Pentadecanone	4.0	11.5	5.5	14.2	5.0	17.6
Coupling ester	3.0	1.3	1.2	1.7	2.9	3.0

Reaction Conditions: 698 K, 1 atm, W/F = 198 g*h/mol, and 25 ml/min of He.

In line with this observation, the ratio of α-olefins to olefins as a function of excess cesium per unit cell is shown in Figure 6.11. It was found that the ratio decrease with increasing excess cesium content in the zeolite. This indicates that amount of excess cesium plays important role in the product distributions from the reaction. It also suggests that the olefins could be derived from the isomerization of

α-olefins by the acid function of the catalyst leading to the increase in the ratio when the excess cesium decreases. This is evidenced by the IR of adsorbed acetonitrile shown in Figure 6.2.

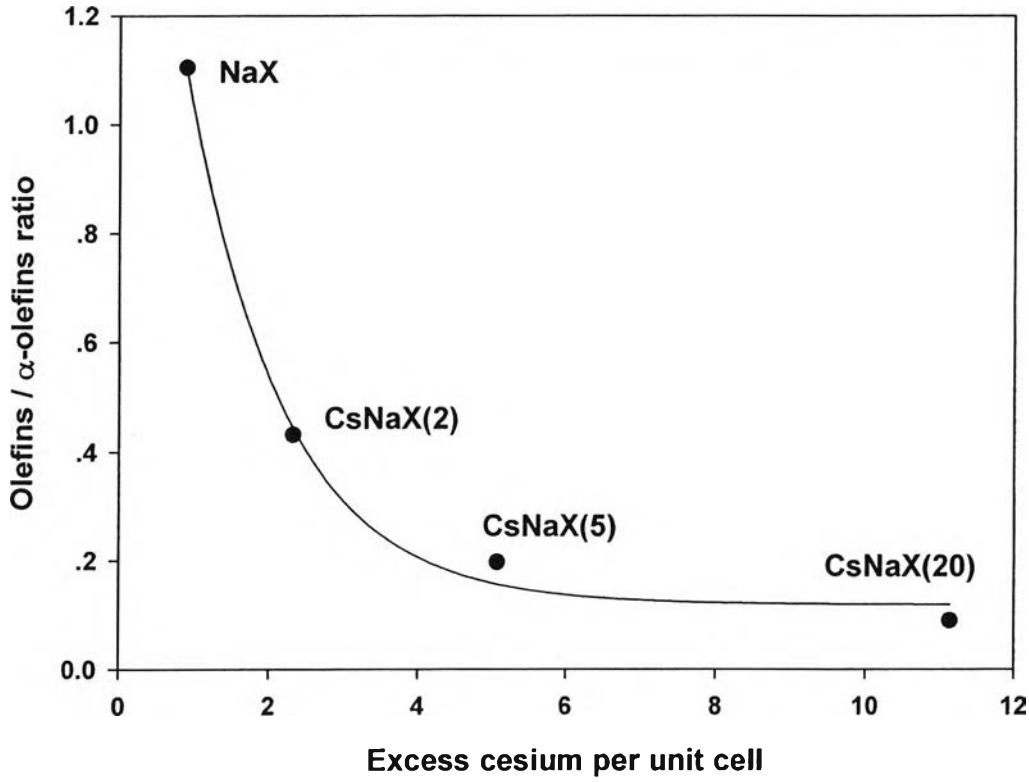

Figure 6.11 The olefins to α-olefins ratio as a function of excess cesium per unit cell.

6.4.4.2 NaX and MgO Catalysts

The deoxygenation activity of methyl octanoate over NaX and MgO catalysts were also studied and compared to that on the CsNaX catalysts. Figure 6.12 illustrates the product distribution obtained over NaX as a function of time on stream, keeping the same conditions as those used over the CsNaX(20) catalysts (compare with Figure 6.8(b)). In significant contrast with the product distribution obtained on the CsNaX(20) catalyst, it was observed that on this catalyst hexenes, heptenes, and multi-substituted aromatics were the dominant products at the beginning of the reaction. Then, as the catalyst deactivated, the aromatic products tended to disappear

and only hexenes and heptenes were obtained as main products at longer time on stream. Moreover, on this catalyst, methanol conversion to dimethyl ether was observed to a significant extent, while absent on the Cs-containing catalyst. Both cyclization and etherification are reactions typically catalyzed by acids, which indicates that the NaX zeolite used in this study contains some acidity, in agreement with previous reports [32].

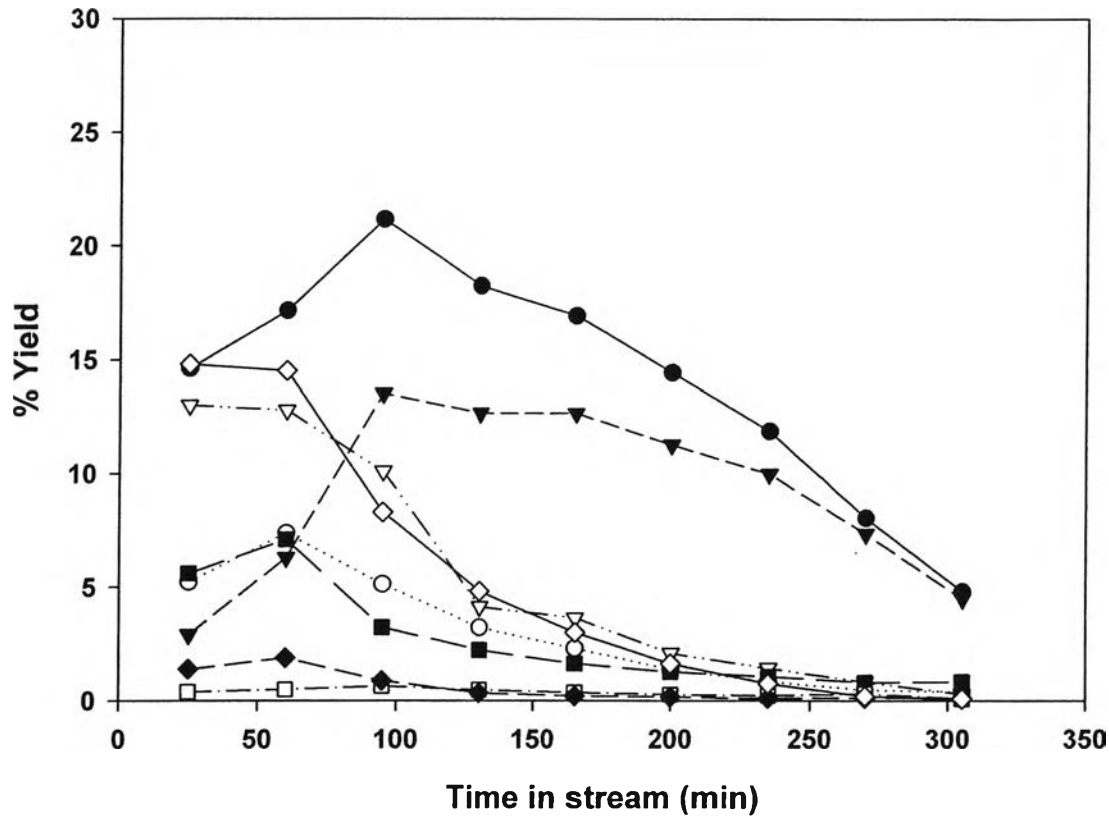

Figure 6.12 Product distribution from the reaction of 10 %wt methyl octanoate in methanol over NaX zeolite catalyst as a function of time on stream. Reaction Conditions: 698 K, 1 atm, W/F = 198 g*h/mol, 25 ml/min of He. Hexenes (●), Heptenes (▼), Multisubstituted aromatics (◇), Heptane (▽), Octenes (■), Hexane (○), Octane (□), and Coupling hydrocarbons (◆).

Also, typical of acid catalysts, rapid deactivation is observed with NaX (see Figure 6.13). As shown below, this deactivation is probably due to coke formation over the acid sites, leading to a more rapid decrease in the production all the acid catalyzed products, namely multi-substituted aromatics, small alkanes, and dimethyl ether. It is interesting that as the acid sites become deactivated, decarbonylation can still proceed and deactivate at a lower rate, leading to a gradual decrease in hexenes and heptenes with time on stream. In line with this concept, the activity of the CsNaX(5) and CsNaX(2) catalysts fall between that of the CsNaX(20) and that of NaX catalysts. Again, the additional (unselective) activity and more rapid deactivation, as compared to the CsNaX(20) catalyst, can be related to the small amount of acid sites generated after the successive washing treatments. This can be evidenced by the IR results of adsorbed acetonitrile shown in Figure 6.2.

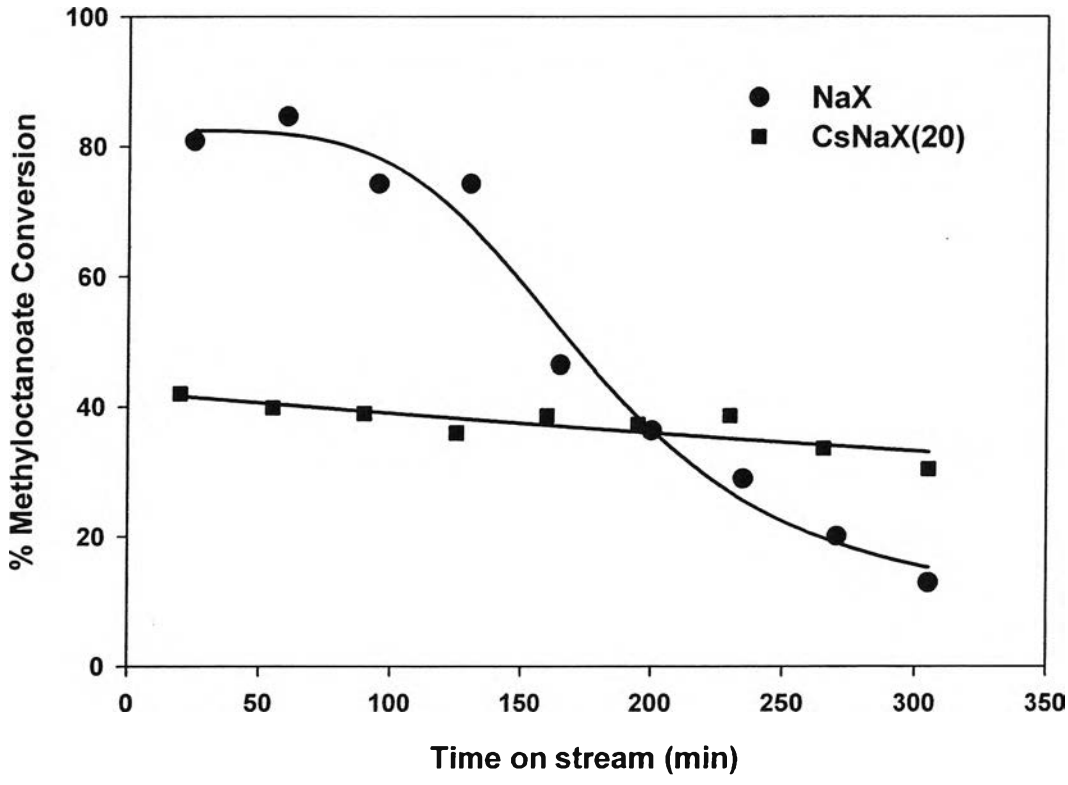

Figure 6.13 Conversion of 10 %wt methyl octanoate in methanol over NaX as a function of time on stream, compared to that on the CsNaX(20) catalyst. Reaction Conditions: 698 K, 1 atm, W/F = 198 g*h/mol, 25 ml/min of He.

To compare to a nonzeolitic basic catalyst, the reaction of 10% methyl octanoate in methanol was investigated under the same conditions as those used for the zeolite catalysts. The conversion and product distribution obtained over this catalyst are shown in Figure 6.14(a) and 6.14(b), respectively. It can be seen that a significantly lower conversion was obtained over MgO compared to that over the CsNaX(20) catalyst. In addition to differences in basicity, the lower catalytic activity of MgO can be attributed to its lower surface area (<40 m^2/g), as compared with that of the zeolites (>400 m^2/g). Moreover, MgO not only shows differences in the activity level, but also in selectivity, which is much lower towards the target hydrocarbon products and higher to undesired condensation products (such as 8-pentadecanone) compared to the high selectivity to C_7-C_8 hydrocarbons displayed by the CsNaX(20) catalyst.

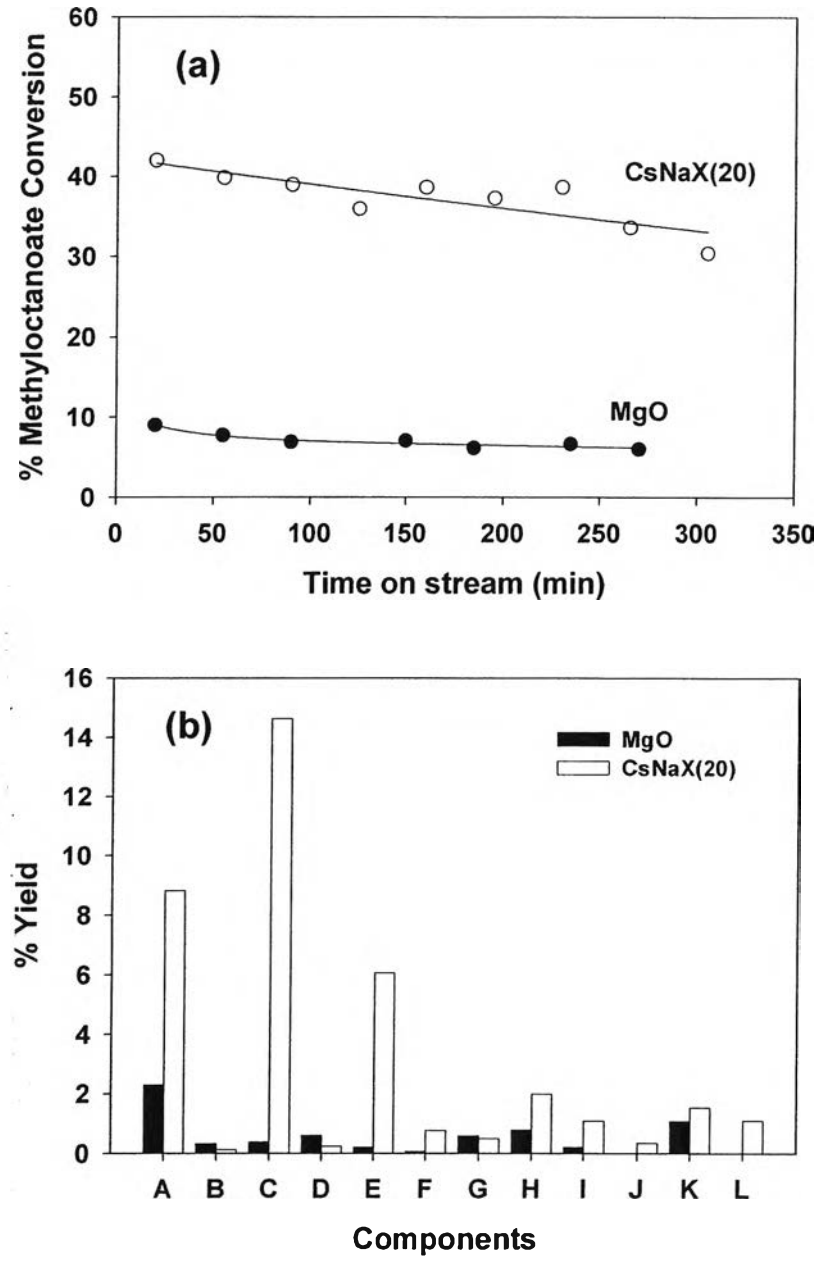

Figure 6.14 Conversion (a) and product distributions (b) of 10 %wt methyl octanoate in methanol from the reaction over the CsNaX(20) and MgO catalysts. Reaction Conditions: 698 K, 1 atm, W/F = 198 g*h/mol, 25 ml/min of He. (A) Hexenes, (B) Hexane, (C) Heptenes, (D) Heptane, (E) Octenes, (F) Octane, (G) Octanal, (H) Oxygenates, (I) Octanoic acid, (J) Tetradecene, (K) Pentadecanone, (L) Coupling ester.

6.4.4.3 CsNaY and Cs/SiO_2 Catalysts

To clarify the role of the excess cesium species, the reaction of methyl octanoate on the Cs/SiO_2 catalysts were carried out at the same conditions. The conversion and the product distribution obtained over the catalyst are illustrated in Figure 6.15. It can be clearly that there is no activity of the methylester taking place over the Cs/SiO_2 catalyst. The very much lower activity of the Cs/SiO_2 catalyst is presumably because of its lower surface area, compared the zeolite catalysts. Although, hexenes were found as main product from the reaction, it was obtained in very low amount. This observation suggests that the excess of cesium species does not play role in the addition decarbonylation or hydrogenation activity of the CsNaX catalysts.

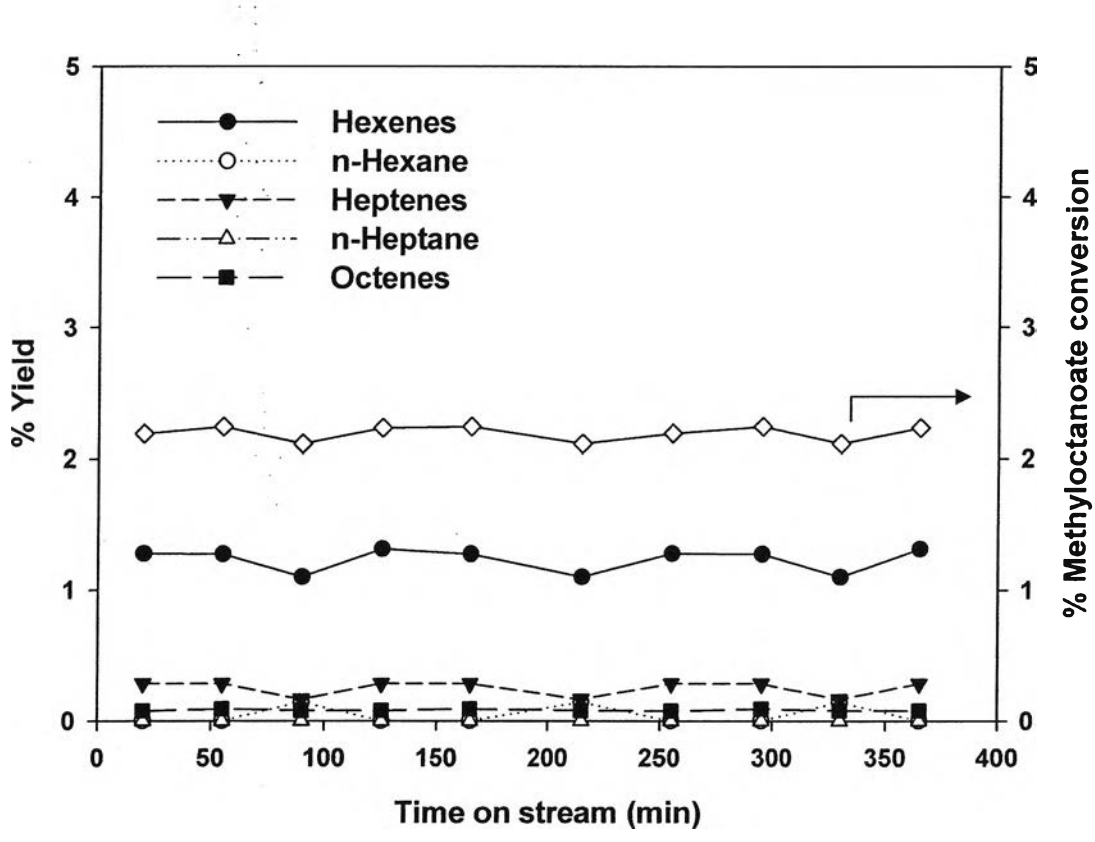

Figure 6.15 Conversion and product distributions of 10 %wt methyl octanoate in methanol over the Cs/SiO_2 catalyst. Reaction Conditions: 698 K, 1 atm, W/F = 198 g*h/mol, 25 ml/min of He.

It is well known that the zeolite Y has the similar pore geometry to the zeolite X. However, the difference in Si/Al of both zeolite results in the difference in the acid-basic characters as mentioned early. To confirm the effect of basic strength, the reaction of 10 %wt of methyl octanoate in methanol was carried out over the CsNaY catalyst under the same conditions. It was found that the catalytic activity of the CsNaY catalyst was similar to that of the CsNaX(20) catalyst as shown in Figure 6.16. In contrast with the product distribution obtained from the CsNaX(20) catalyst, it showed that the CsNaY catalyst yieled the hexens as the main products followed by the heptenes during the reaction period. This observation may be attributed to the decrease in the basic strength of the CsNaY, compared to the CsNaX(20) catalysts as shown in Figure 6.2.

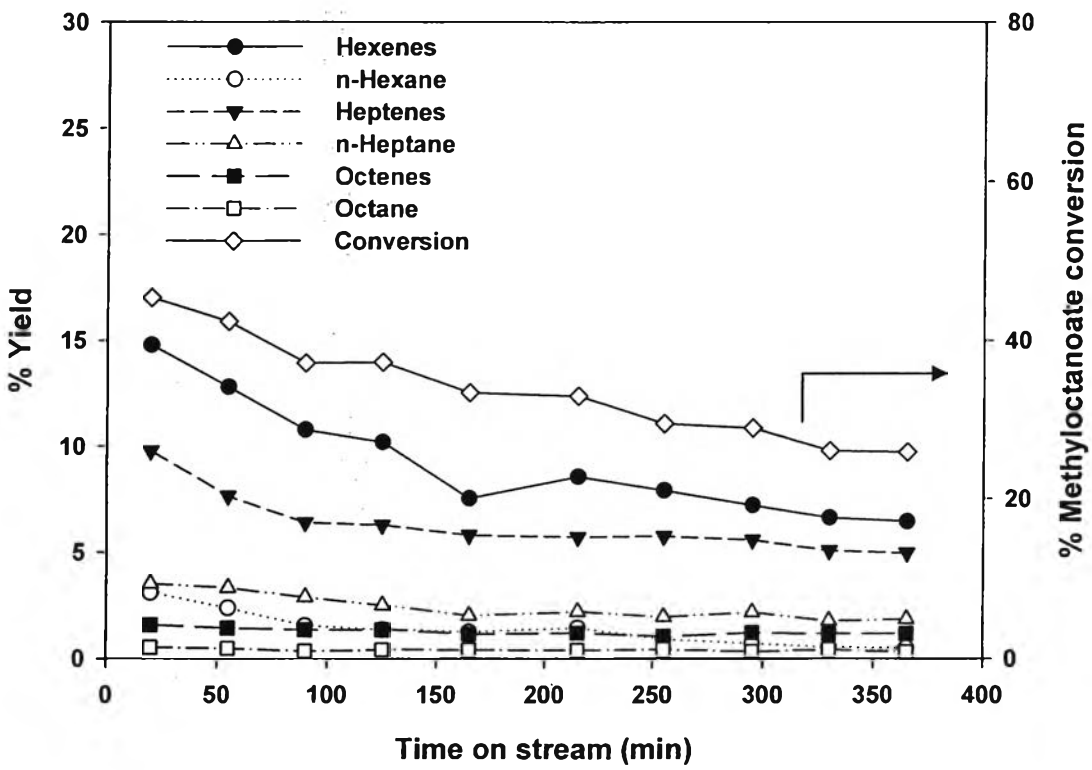

Figure 6.16 Conversion and product distributions of 10 %wt methyl octanoate in methanol over the CsNaY catalyst. Reaction Conditions: 698 K, 1 atm, W/F = 198 g*h/mol, 25 ml/min of He.

6.4.5 Characterization of Spent Catalysts

The coke residues left on the catalysts after the conversion of methyl octanoate were quantified by TPO. Figure 6.17 shows that when nonane was used as a solvent, more than twice as much coke was deposited on the CsNaX(20) catalyst as when methanol was used. This difference in coke deposition explains the different deactivation rates observed when nonane was used instead of methanol as solvent. It can also be seen that the oxidation of the deposits from these reactions appeared at a relatively lower temperature (~553 K), as compared to that of conventional hydrocarbon coke deposites (>823 K). This suggests that the deposits on the CsNaX(20) are mainly high-molecular-weight oxygenates rather than the typical polynuclear aromatic coke.

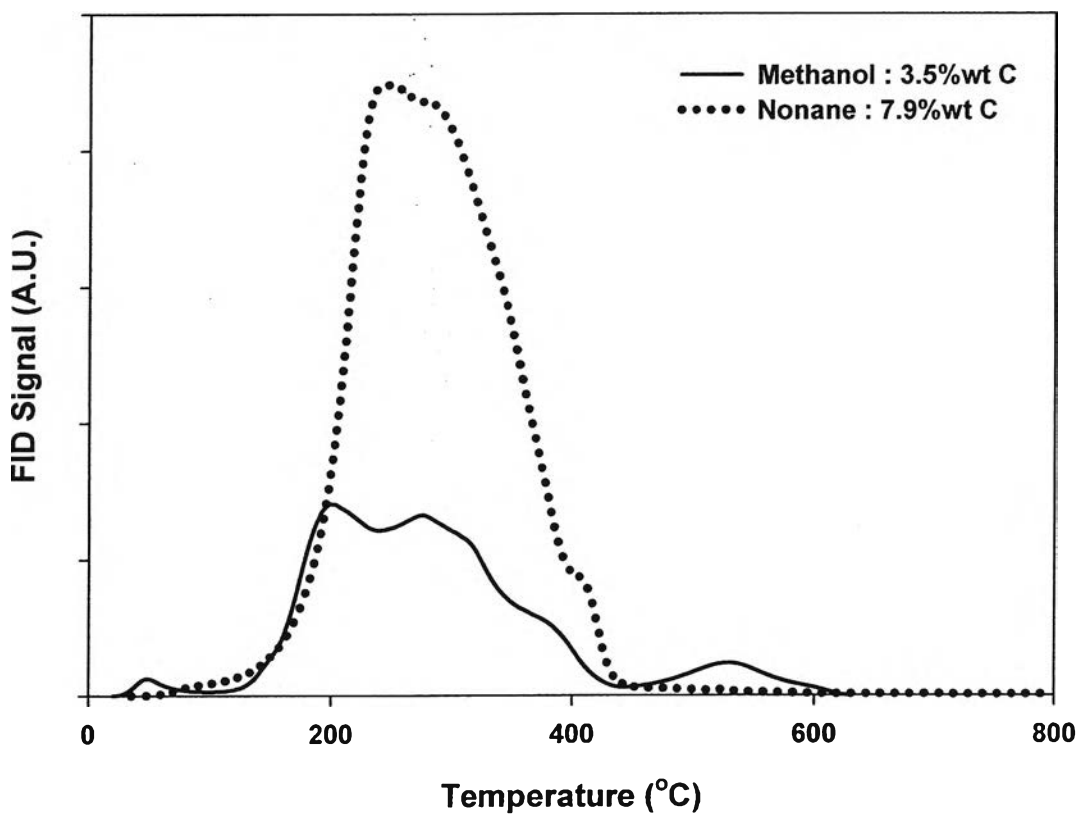

Figure 6.17 TPO profiles of the spent CsNaX(20) catalysts from the reaction of 10 %wt methyl using nonane and methanol as solvent.

Figure 6.18 shows the TPO profiles of the coke deposited during the reaction of 10% methyl octanoate in methanol over NaX, compared to the CsNaX(20) catalyst. It is clear that on NaX not only a significantly higher amount of deposits was formed, but also there is an important fraction of the deposits that decomposes at significantly higher temperature (623 K), as compared with that in the CsNaX(20) catalyst. In line with the concepts discussed above, this additional deposit may be derived from the residues resulting from acid-catalyzed reactions. While the oxidation temperature of these species is higher than that observed with the basic CsNaX catalyst, it is much lower than that typically observed over strong acid catalyst. Hence, these deposits should not be referred to as polynuclear aromatic coke, but rather as oxygenated aromatic compounds formed over the weak acid sites of NaX.

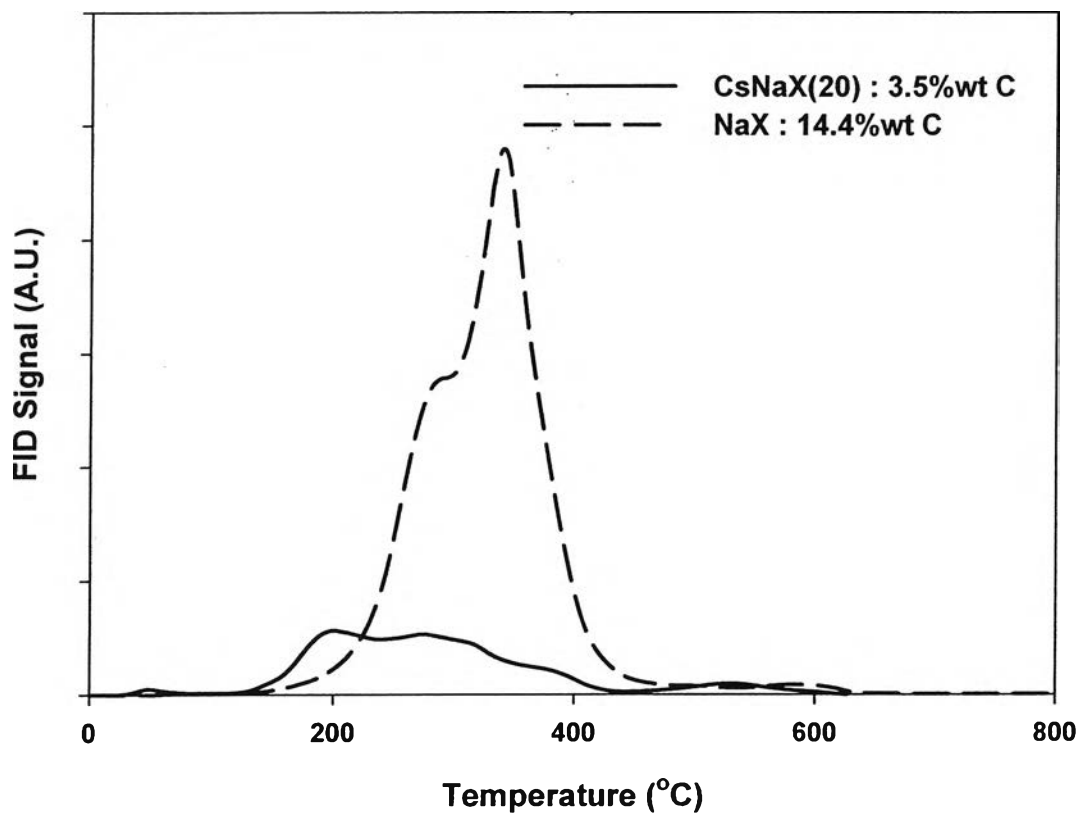

Figure 6.18 TPO profiles of the spent CsNaX(20) and NaX catalysts from the reaction of 10 %wt methyl octanoate in methanol.

6.5 Discussion

The rapid deactivation of the CsNaX(20) zeolite catalyst observed during the reaction of methyl octanoate in nonane is presumably due to the adsorption of methyl octanoate on the highly basic sites of the zeolite that may not be greatly affected by the presence of the hydrocarbon solvent. Such strong adsorption may lead to a rapid deactivation by site (and probably pore) blockage. Under these conditions, the adsorbed methyl octanoate can react with each other (self-condensation) forming the observed high-molecular-weight oxygenates (e.g. 8-pentadecanone). Such compounds cannot readily diffuse out from the pores of the zeolite and lead to further blockage. The formation of high-molecular weight products is usually derived from (i) condensation (mostly aldol type) of the carbanion intermediates with available electrophilic species [33], or (ii) self-condensation [34]. It must be noted that these coupling products do not necessarily form a hard coke, since, as the TPO results show, they can be removed at relatively low oxidation temperatures (i.e. below 573 K).

By contrast, the use of methanol as a solvent generates a completely different situation. First, the catalytic stability of the CsNaX(20) catalyst is greatly enhanced. Methanol being a highly polar molecule it can competitively interact with the zeolite basic sites [18]. Several reports [35,36] have suggested that adsorption of methanol derives mainly from interactions between the methoxyl oxygen and the exchangeable cation and interactions between the hydroxyl hydrogen and the framework oxygen.

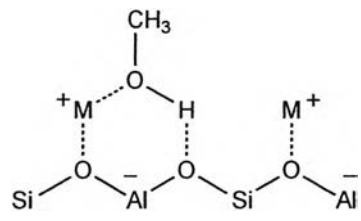

When M^+ is Cs^+, a highly polarizable cation, the interaction between M^+-O is relatively weaker than that with higher Lewis acid Na^+. However, over CsNaX, the framework O-H interaction become stronger and hence this weaken the O-H of

methanol. As shown in the TPD and TPRx studies, this interaction leads to the decomposition of methanol to yield primarily a surface COH_2 and hydrogen. The surface COH_2 would then form a formate-like species, which can be further converted into a carbonate-like species as the temperature increases, as evidenced by NMR signals at 166 and 171 ppm, respectively [30].

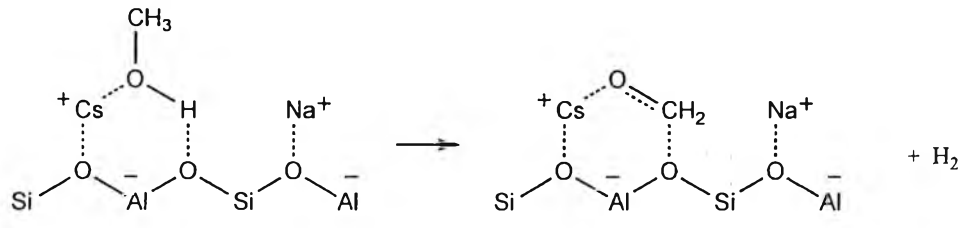

formate-like species (^{13}C NMR signal ~166 ppm)

Under our reaction conditions, we expect both surface formate and surface carbonate species will be present. These species can readily compete with the adsorption of methyl octanoate, thus lowering its surface coverage and inhibiting the self-condensation reaction. As a result, this adsorption inhibition suppresses the formation of high-molecular weight oxygenates, resulting in better catalytic stability. Also, consistent with the above discussion, a lower initial activity can be expected for the reaction in the presence of methanol, as experimentally observed. Since there is no significant difference in activity and product selectivity when hydrogen is used as carrier gas, we may suggest that the hydrogen, produced *in situ* from the methanol decomposition, can further facilitate the hydrogenation of methyl octanoate and its primary products. Hence, various olefins and alkanes, such as octene, hexane and heptane were obtained from the reaction using methanol as a solvent.

As suggested by TPD results (Figure 6.6), the methyl octanoate is strongly adsorbed on basic sites of the CsNaX(20) catalyst. Due to the highly polarizable nature of methyl octanoate, the interaction between carbonyl ester and the basic framework oxygen would readily weaken the carboxylic C-O bond, leading to the decomposition of the ester into two surface-aldehydes, as generally observed over typical basic catalysts [37]. In this case, the decomposed methoxyl group would also form the formate-like species (surface-formaldehyde) while the other fragment would form an "octanoate-like species" (surface-octanaldehyde), in parallel with the

formation of the formate-like species discussed above. This formate-like species would then decompose into carbon monoxide and hydrogen, in a manner similar to that observed with methanol. This primary decomposition of the methoxyl group is evidenced in the present study by the observed CO evolution prior to the formation of hydrocarbon (~573-673 K). The fact that the amount of CO evolved at this temperature range (~1.6 μmol/g) is relatively small compared to that evolved at higher temperatures (~6.8 μmol/g), suggests that the decomposition of the formate-like species was not the dominant path, but the species was retained on the surface up to higher temperatures.

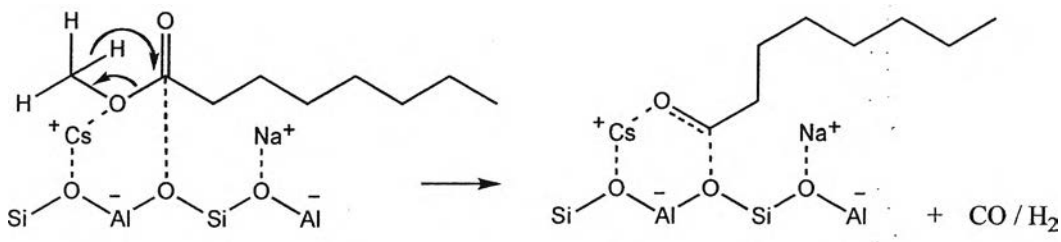

It is proposed that decomposition of such "octanoate-like species" leads to the formation of the two major hydrocarbon products observed on the CsNaX(20) catalyst, heptene and hexene. In the first case, the well-known β-hydrogen elimination [38] and subsequently decomposition would result in heptene as major product of the reaction, with parallel evolution of CO and H_2. This reaction may well be referred to as a reversible reaction of the typical hydroformylation [39]. In the second case, the decomposition of a cyclic-like intermediate can lead to the formation of more electrophilic acetaldehyde (enol-form) and hexene, as shown below. The acetaldehyde may be evolved as a by-product or may undergo further aldol condensation / alkylation to form C3-C5 oxygenates, as observed in small amounts by GC-MS.

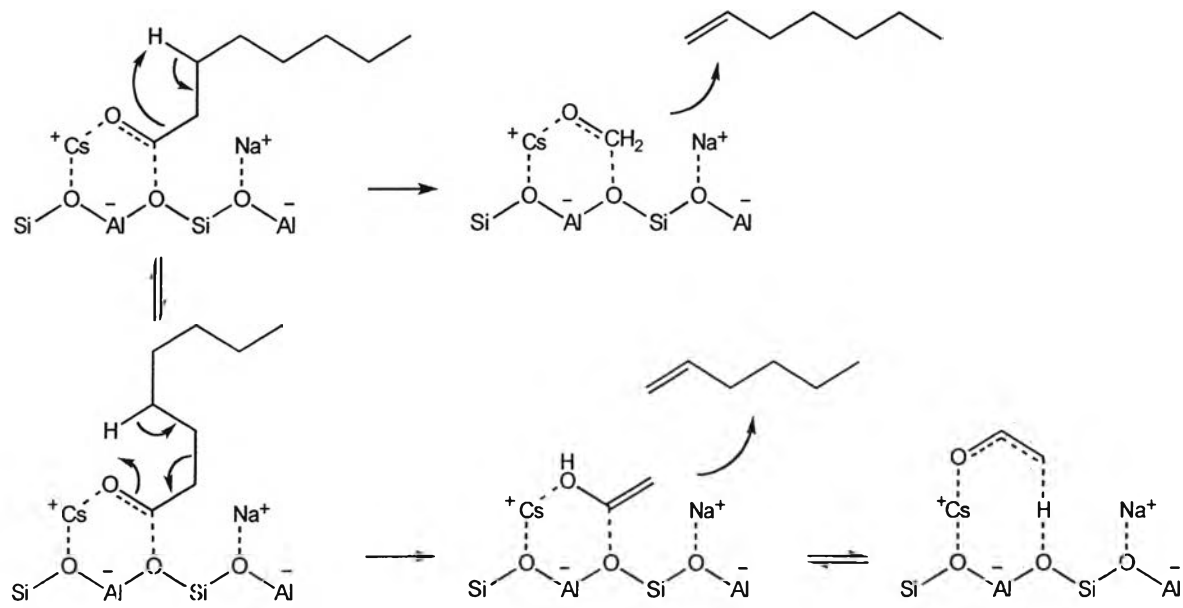

It must be noted that while hydrogen is not essentially required for the production of heptenes and hexenes it is necessary for the formation of octenes and alkanes via hydrogenation/dehydration. These reactions can indeed occur on cesium-exchanged zeolites [40]. As discussed above, due to the highly polarizable cesium cations, the basic sites associated with it can readily decompose the methanol / methoxyl group, creating a hydrogen surface fugacity well above that in equilibrium with hydrogen in the gas phase [41,42]. With such high virtual pressure of hydrogen, the adsorbed "octanoate-like species" may well be hydrogenated forming primarily an octanol that then rapidly undergoes dehydration to form octenes.

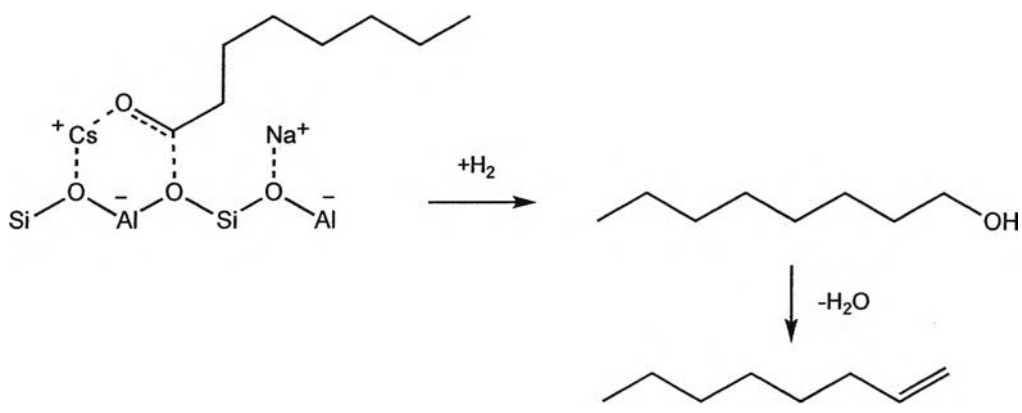

The small amounts of octane, heptane and hexane in the product give evidence for the hydrogenation activity of the CsNaX(20) catalysts (see Table 6.2). However, the extent of this reaction is small in comparison to that of the octanoate-like species decomposition. This is because olefins are less adsorptive on the basic sites, as compared to the more electrophilic octanoate-like species. These hydrogenolysed / hydrogenated products can be particularly promoted in the reaction with methanol, but not readily with nonane (Figure 6.8).

A higher amount of hexenes and hexane observed from the CsNaX(2) and CsNaX(5) catalysts, compared to the CsNaX(20) catalyst give an evidence for the additional acidity of the CsNaX(5) and CsNaX(2) catalysts. This is because the CsNaX(5) and CsNaX(2) catalysts contain less excess cesium per unit cell leading to the decrease in the basic strength and the increase in the acidity of the Lewis sites in the zeolites, as evidenced by the shift of the acetronitrile adsorption band to lower frequency. Hence, the hexenes yielded from the reaction over the CsNaX(2) and CsNaX(5) were obtained from the decomposition of the cyclic-like species on the catalyst surface taking place on the acid sites. Consistent with this view, hexenes were obtained as a main product over the CsNaY catalyst, which contains same pore structure as the CsNaX catalysts but different basic-acid character. A higher ratio of olefins to α-olefins was observed when the excess cesium decreased. This indicates the isomerization over the acid sites of the CsNaX(5) and CsNaX(2) catalysts. Moreover, it must be noted that the excess cesium cation does not provide any additional decarbonylation and hydrogenation activity of the CsNaX catalysts as shown by the activity over the Cs/SiO_2. It suggests that the role of the excess cesium cation is to provide more Lewis basicity to the zeolites.

The observed small amounts of 8-pentadecanone and long-chain olefins suggest another reaction path on the CsNaX(20) catalysts. We believe that 8-pentadecanone is not derived from the "octanoate-like" intermediate responsible for the production of heptenes and hexene. Instead, this large product is likely to arise from the decomposition of an acid anhydride. The adsorbed methyl octanoate may undergo a condensation reaction, forming dioctanoic acid anhydride. The acid anhydride may undergo a decarboxylation to ketone [43] on the basic sites since the highly negative framework charge of oxygen would act as an acceptor for the acidic

CO_2. This path would explain the high yield of 8-pentadecanone observed in the reaction when nonane is used as a solvent.

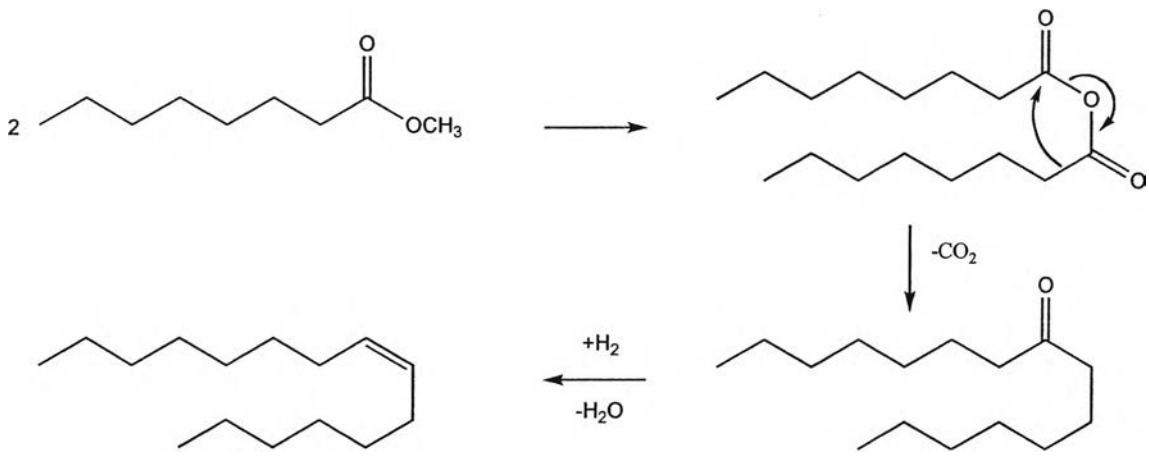

Due to its low mobility, 8-pentadecanone is likely to stay on surface long enough to be hydrogenated by the adsorbed H to form alcohol, but such a heavy alcohol would undergo dehydration, forming a long-chain inner olefin. In fact, as W/F increases, 8-pentadecanone is seen to be readily converted and this is consistent with the observed increase in the yields of long-chain olefins at longer space times.

The comparison of the catalytic behavior of the CsNaX(20) catalyst with those of NaX and MgO indicates that the presence of polarizable Cs cations result in a catalyst with unique performance. First, on these catalysts, the decarbonylation / deacetalation activity is not as pronounced as over the CsNaX(20) catalyst. Also, since the Na cation is much harder than the Cs cation [44] it holds the negative framework charge more tightly and thus it provides less Lewis basicity to the framework oxygen [45]. That is, the presence of Na as exchangeable cation, leads to an increase in the (weak) acidity of the Lewis sites in the zeolite, as evidenced by IPA-TPD. This weak acidity would explain the formation of aromatic products and the rapid deactivation over NaX. Consistent with this view, a higher amount of coke deposits was found on NaX, with an important fraction of the carbonaceous species decomposed at relatively high temperature (Figure 6.18).

It should be noted that the yield of hexene is higher than that of heptene over NaX, but the opposite is true for the CsNaX(20) catalyst. This difference suggests that in the case of NaX additional hexenes are produced by cracking of higher molecular weight compounds, not only from the deacetalation that occurs in the CsNaX(20) catalyst. The additional yields due to cracking would also be applied to heptene and other hydrocarbons formed, and hence these reactions give a higher initial conversion over this catalyst. It is also interesting to note that, after the weak acid sites are deactivated in NaX, the production of heptene and hexene slowly decreases with time on stream (Figure 6.12). As proposed above, these products arise from both cracking over acid sites and by decarbonylation / deacetalation over basic sites. As the acid sites are deactivated while the latter are still active, a gradual decrease only in these two products with time on stream is observed. Accordingly, since after about 250 minutes on stream the acid function has been completely eliminated, the residual activity can be ascribed to the decarbonylation / deacetalation activity of NaX.

The suggestion that the alkali-exchanged zeolites contain both acid and basic functions, is in agreement with earlier studies [46,47] that indicate that NaX can be regarded as an amphoteric catalyst, interacting with polar oxygenates in a manner totally different from that observed over the CsNaX(20) catalyst. For example, over NaX, methanol competes with methyl octanoate for adsorption and consequently DME is largely produced by dehydration of methanol. Also, on this catalyst, in addition to decarbonylation, methyl octanoate undergoes acid-catalyzed reactions, such as cracking, isomerization, alkylation, dimerization, and even aromatization. Hence, multi-substituted aromatics are obtained over NaX since methanol can readily act as a methylating agent over weakly acidic sites. When the acid sites are deactivated, the cracking products and aromatics virtually disappear. Only decarbonylation and deacetalation activity due to negative framework charge of NaX remains. However, this is to a much lower extent than on the CsNaX(20) catalyst. In addition, it can be seen that on NaX, without Cs, no hydrogenation activity can be observed and the use of methanol as a solvent, does not facilitate the maintenance of the desirable reactions.

By analyzing the behavior observed on the MgO catalyst, one can conclude that not only the basicity is required for decarbonylation, but also the highly polar environment of the zeolite micropore seems to play an essential role in adsorption and decomposition of the adsorbed species. Although MgO is well regarded as a highly basic catalyst, its two dimensional surface cannot readily facilitate the adsorption and decomposition of methyl octanoate. In addition, a much lower surface area, as compared to that of the zeolites, would show a significant effect on activity. Hence, on this catalyst only small amounts of deoxygenate products were obtained, as compared to that on the CsNaX catalysts. By contrast, the MgO catalyst seems to display enough basicity to activate the coupling reaction of methyl octanoate, thus resulting in the formation of 8-pentadecanone. As mentioned above, the 8-pentadecanone is formed via the decomposition of an acid anhydride intermediate. As the acid anhydride is a "hard" species, it would possess a better interaction and decomposition to 8-pentadecanone over the "hard" MgO base.

While MgO can readily decompose methanol to CO and H_2 [48], small amounts of octene and hydrogenated products can be found over this catalyst. It is believed that the absence of highly polarisable cesium cation and the highly polar environment in restricted pore of the zeolites, reduce its ability to adsorb and dissociate hydrogen. Therefore, hydrogenation cannot be readily promoted and yields of octene, heptane and hexane are relatively small.

6.6 Conclusions

It can be concluded that the decarbonylation / deacetalation activity of methyl octanoate can occur at high rate and for a long time on stream over CsNaX when co-feeding methanol. Methyl octanoate strongly adsorbs on CsNaX, basic sites and cannot be desorbed unless decomposed. When a weak adsorbent as nonane is co-fed CsNaX rapidly deactivates. By contrast, when methanol is co-fed with methyl octanoate the catalyst stability is greatly enhanced due to the presence of decomposed fragments of methanol on the surface. These fragments are formate-like species that prevent self-condensation and formation of higher molecular weight oxygenates. The TPD results suggest that the decarbonylation of methyl octanoate

proceeds via primary decomposition at the methoxyl group, presumably producing an octanoate-like species as intermediate. The direct decomposition of this species gives heptenes and hexenes as main products. Octenes and other hydrogenated products are formed by hydrogenation / dehydration, in which the surface hydrogen produced from methanol decomposition plays an important role.

Role of cesium is to provide the basicity to the zeolite catalysts. When Cs is not present (NaX zeolite) the catalyst basicity is much lower and the weak acid sites dominate the behavior of the catalyst. The net results are a decrease in the decarbonylation / deacetalation activity, together with an increase in the selectivity toward undesired products. The poor performance displayed by the MgO catalyst indicates that not only the basicity is required for decarbonylation, but also the highly polar environment characteristic of the zeolite micropore seems to play an essential role.

6.7 Acknowledgments

This work was financially supported by the Oklahoma Secretary of Energy, the Oklahoma Bioenergy Center, Thailand Research Fund under the Royal Golden Jubilee Ph.D. Program, the Center for Petroleum, Petrochemicals, and Advanced Materials (PPAM), and the Petrochemical and Environmental Catalysis Research Unit of the Ratchadapiseksompote Endowment. The authors would like to thank Assoc. Prof. Tawan Sooknoi for his helps and suggestions and Mr. Surapas Sitthisa for TPO analysis.

6. 8 References

[1] D. E. Lopez, K. Suwannakarn, D. A. Bruce, J. G. Goodwin Jr., *J. Catal.* 247 (2007), 43

[2] I. N. Martyanov, A. Sayari, *Appl. Catal. A* 339 (2008) 45

[3] D. A. G. Aranda, R. T. P. Santos, N. C. O. Tanpanes, A. L. D. Ramos, O. A. C. Antunes, *Catal. Lett.* 122 (2008) 20

[4] M. D. Serio, R. Tesser, L. Pengmei, E. Santacesaria, *Energy and Fuels* 22 (2008) 207

[5] G. Knothe, *Fuel Process. Technol.* 86 (2005) 1059

[6] G. Knothe, A. C. Matheaus, T. W. Ryan III, *Fuel* 82 (2003) 971

[7] G. Knothe, *Fuel Process. Technol.* 88 (2007) 669

[8] W. F. Maier, P. Grubmiller, I. Thies, P. M. Stein, M. A. McKervey, P. R. Schleyer, *Angew. Chem. Int. Ed.* 18 (2003) 939

[9] D. S. Brands, G. U-A-Sai, E. K. Poels, A. Bliek, *J. Catal.* 186 (1999) 169

[10] T. A. Foglia, P. A. Barr, *J. Am. Oil. Chem. Soc.*, 53 (1976), 737

[11] I. Kubickova, M. Snare, K. Eranen, P. Maki-Arvela, D. Y. Murzin, *Catal. Today*, 106 (2005) 197

[12] P. Maki-Arvela, I. Kubickova, M. Snare, K. Eranen, D. Y. Murzin, *Energy Fuels*, 21 (2007) 30

[13] M. Snare, I Kubickova, P. Maki-Arvela, K. Eranen, J. Warna, D. Y. Murzin, *Chem. Eng. J.* 134 (2007) 29

[14] G. N. Rochafilho, D. Brodzki, G. Djega-Mariadassou, *Fuel* 72 (1993) 543

[15] M. Snare, I. Kubickova, P. Maki-Arvela, D. Chichova, K. Eranen, D. Y. Murzin, *Fuel* 87 (2008) 933

[16] I. Rodriguez, H. Cambon, D. Brunel, M. Lasperas, *J. Mol. Catal. A-Chemical,* 130 (1998) 195

[17] X. F. Zhang, E. S. M. Lai, R. Martin-Aranda, K. L. Yeung, *Appl. Catal. A-General* 261 (2004) 109

[18] T. Sooknoi, J. Dwyer, *J. Mol. Catal. A: Chem.* 211 (2004) 155

[19] P. Belirame, P. Fumagallip, G. Zuretti, *Ind. Eng. Chem. Res.* 32 (1993) 26

[20] D. Barthomeuf, *Catal. Rev.* 38 (1996) 521

[21] M. Lasperas, H. Cambon, D. Brunel, I. Rodriguez, P. Geneste, *Microporous Materials*, 7, 61 (1996)

[22] U.D. Joshi , P.N. Joshi, S.S. Tamhankar, V.V. Joshi, C.V. Rode, V.P. Shiralkar, *Appl. Catal. A: Gen.* 239 (2003) 209

[23] Y. Sun, Z. Liu, P. Pianetta, D. Lee, *J. Appl. Phys.* 102 (2007) 074908

[24] E. A. Podgornov, I.P. Prosvirin, V. I. Bukhtiyarov, *J. Mol. Catal. A: Chem.* 158 (2008) 337

[25] T. Sooknoi, J. Dwyer, *J. Mol. Catal. A: Chem.* 211 (2004) 155.

[26] R. Schenkel, A. Jentys, S. F. Parker, J. A. Lercher, *J. Phys. Chem. B* 108 (2004) 7902

[27] N. Takahashi, A. Mijin, T. Ishikawa, K. Nebuka, H. Suematsu, *J. Chem. Soc., Faraday Trans. I,* 83 (1987) 2605

[28] F. Yagi, H. Tsuji, H. Hattori, *Microporous Mater.* 9 (1997) 237

[29] S. Imamura, T. Higashihara, Y. Saito, H. Aritani, H. Kanai, Y. Matsumura, N. Tsuda, *Catal. Today*, 50 (1999) 369

[30] M. Hunger, U. Schenk, M. Seiler, J. Weitkamp, *J. Mol. Catal. A: Chem.* 156 (2000) 153

[31] G. W. Huber, A. Corma, *Angew. Chem. Int. Ed.* 46 (2007) 7184

[32] H. B. Schwarz, S. Ernst, J. Karger, B. Knorr, G. Seiffert, R. Q. Snurr, B. Staudte, J. Weitkamp, *J. Catal.* 167 (1997) 248

[33] J. Li, J. Tai, R. J. Davis, *Catal. Today*, 116 (2006) 226

[34] N. D. Plint, N. J. Coville, D. Lack, G. L. Nattrass, T. Vallay, *J. Mol. Catal. A: Chem.* 165 (2001) 275

[35] D. F. Plant, A. Simperler, R. G. Bell, *J. Phys. Chem. B* 110 (2006) 6170

[36] P. Mignon, P. Geerling, R. Schoonheydt, *J. Phys. Chem. B* 110 (2006) 24947

[37] H. N. Wright Jr., H. J. Hagemeyer Jr., US Patent 3,714,236 (1973)

[38] N. Takahashi, H. Matsuo, M. Kobayashi, *J. Chem. Soc., Faraday Trans. 1*, 80 (1984) 629

[39] G. Cuma, P. Famulari, M. Marchetti, B. Sechi, *J. Mol. Catal. A: Chem.* 218 (2004) 211

[40] T. Sooknoi, J. Dwyer, *Stud. Surf. Sci. Catal.* 97 (1995) 423

[41] E. Iglesia, J. E. Baumgartner, G. L. Price, *J. Catal.* 134 (1992) 549

[42] M. Boudart, *Catal. Lett.* 3 (1989) 111

[43] M. Glinski, W. Szymanski, D. Lomot, *Appl. Catal. A* 281 (2005) 107

[44] R. G. Pearson, *J. Am. Chem. Soc.* 85 (1963) 3533

[45] Y. Okamato, M. Ogawa, A. Maezawa, T. Imanaka, *J. Catal.* 112 (1988) 427

[46] F. Horst, F. Hartmut, G. Ekkehard, H. Bernd, J. Herve, K. Christine, K. Olaf, K. Knut, *Phys. Chem. Chem. Phys* 1 (1999) 593

[47] J. A. Lercher, A. Jentys, A. Brait, *Mol. Sieves. Sci. Tech.* 6 (2008) 153

[48] D. C. Foyt, J. M. White, *J. Catal.* 47 (1977) 260